Influence of Intercritical Austenitizing Temperature, Quenching Media and Tempering Temperature on Mechanical Properties and Wear Behavior of Ductile Iron with Dual Matrix Structure

Dissertation submitted to the

National Institute of Technology Rourkela

in partial fulfillment of the requirements

of the degree of

Master of Technology (Research)

in

Metallurgical and Materials Engineering

by

Yahya Hoque Mozumder

(Roll Number: 612mm3010)

under the supervision of

Prof.Sudipta Sen

December, 2015

Department of Metallurgical and Materials Engineering

National Institute of Technology Rourkela

Metallurgical and Materials Engineering
National Institute of Technology Rourkela

December 23, 2015

Certificate of Examination

Roll No: 612MM3010

Name: Yahya Hoque Mozumder

Title of Dissertation: Influence of Intercritical Austenitizing Temperature, Quenching Media and Tempering Temperature on Mechanical Properties and Wear Behavior of Ductile Iron with Dual Matrix Structure

We the below signed, after checking the dissertation mentioned above and the official record book (s) of the student, hereby state our approval of the dissertation submitted in partial fulfillment of the requirements of the degree of Master of Technology (Research) in Metallurgical and Materials Engineering at National Institute of Technology Rourkela. We are satisfied with the volume, quality, correctness, and originality of the work.

APPROVED

…….
S Sen
Associate Professor, MM Department
(Principal Supervisor)

…….
S Chaudhuri
Retd. Scientist (G), NML India
(External Examiner)

…….
S K Patel
Associate Professor, ME Department
(MSC Member)

…….
A Satapathy
Associate Professor, ME Department
(MSC Member)

…….
S C Mishra
Professor& HOD, MM Department
(Chairman, MSC)

Metallurgical and Materials Engineering
National Institute of Technology Rourkela

Prof. Sudipta Sen

Associate Professor
Metallurgical and Materials Engineering
National Institute of Technology Rourkela

December 23, 2015

Supervisor's Certificate

This is to certify that the work presented in this dissertation entitled *"Influence of Intercritical Austenitizing Temperature, Quenching Media and Tempering Temperature on Mechanical Properties and Wear Behavior of Ductile Iron with Dual Matrix Structure*" by "*Yahya Hoque Mozumder*", Roll Number 612MM3010, is a record of original research carried out by him under my supervision and guidance in partial fulfillment of the requirements of the degree of *Master of Technology* in *Metallurgical and Materials Engineering*. Neither this dissertation nor any part of it has been submitted for any degree or diploma to any institute or university in India or abroad.

Sudipta Sen

DEDICATION

I dedicate this thesis to my family for nursing me with affections and love and their dedicated partnership for success in my life

Acknowledgement

At final steps towards my M. Tech (Research) degree I would like to acknowledge so many people and institution that have made this journey possible. First of all, it's a privilege for me to express my profound gratitude and indebtedness to my supervisor Dr. Sudipta Sen, Metallurgical & Materials Engineering Department, National Institute of Technology Rourkela. Without his efforts and guidance this work could not have been possible. He has guided me at all stages during this research work. I will cherish all the moments of enlightenment he has shared with me.

I would like to convey my sincere gratitude to Prof. S. C. Mishra, Head of the Department, Metallurgical and Materials Engineering Department, National Institute of Technology Rourkela, for constant guidance and encouragement. I am also grateful to my Master Scrutiny Members: Dr. Saroj Kumar Patel and Dr. Alok Satapathy from the Mechanical Department of the National Institute of Technology Rourkela. Thank you so much for your valuable input and advice during the research work.

My appreciation goes to the entire Metallurgical and Materials Engineering faculty and staff for all their help along the way. I would like to thank especially Mr. S. Hembram for performing me the tensile test of the specimens, Mr. S. Pradhan for helping in taking SEM images and Mr. Arindam Pal to carry out my XRD test.

I would like to thank the National Institute of Technology Rourkela for allowing me to come to NIT to pursue my M. Tech (Research) Degree.

I would like to acknowledge my beloved friends Ranjan, Lailesh, Ajit, Abhinay, and Harshpreet for their unconditional help and support during my research work. Thank you all for the good times we have had together.

I would like to especially acknowledge my sisters for their love, affection and understanding me along the way. Special thanks to my parents for their unconditional love and motivating me and assisting me through my life. Without their help and encouragement it would not have been possible for me to undertake this work.

December 23, 2015 **Yahya Hoque Mozumder**

NIT Rourkela **Roll No 612MM3010**

CONTENTS

List of Figures

List of Tables

Abstract

Mechanical properties of ductile iron are controlled primarily by the distribution and amount of matrix phases and micro-constituents. In the moderately newly developed ductile iron with dual matrix, the structure consists of ferrite (soft phase) and martensite (hard phase) which is called dual matrix structure. This structure is obtained by a special heat treatment process in which the ductile iron is subjected to an incomplete austenitization stage within the intercritical intervals followed by a fast cooling step to transform austenite into martensite. Ductile iron with dual matrix structure holds promises for the production of suspension parts for automotive industries and safety components for military industries where high strength and ductility is required. The further development and applications of intercritical heat treatments in ductile iron requires an increasing understanding of different aspects of this kind of heat treatment cycle. The present dissertation was focused on studying the influence of intercritical austenitizing temperature, quenching media and tempering temperatures on mechanical properties and wear behavior of dual matrix structured ductile iron.

Ductile iron (3.56 C wt. %, 2.07 Si wt. %, 0.17 Mn wt. %) was intercritically austenitized in two phase region ($\alpha + \gamma$) at temperatures of 785°C and 815°C for 5 minutes and then quenched in two different quenching media paraffin liquid light oil and water to obtain dual matrix structured ductile iron with different ferrite and martensite volume fractions. Some specimens were quenched from same intercritical austenitizing temperatures and tempered for 1 hour at three different tempering temperatures of 400°C 450°C and 500°C to produced quenched and tempered dual matrix structured ductile iron. The microstructures of all the treated ductile iron samples were analyzed using optical microscopy and metal pro image analyzer. X-Ray diffraction of dual matrix structured ductile iron was done for the phase detection. To study the mechanical properties tensile test were performed by using Instron 1195 and hardness

measurement was determined using Vickers hardness tester. Fractographic analysis of tensile fractured surface was done using field emission scanning electron microscopy. Wear properties of all the treated ductile iron samples was analyzed by using a ball-on-plate tribometer. The worn surface was studied under scanning electron microscopy in order to study the wear mechanism involved.

The result shows that volume fraction of martensite and ferrite can be controlled to obtain the strength and ductility of ductile iron with dual matrix structure. The weight loss resistance and strength increased and ductility decreased with increased martensite volume fraction. The ultimate tensile strength and yield strength initially drops and remains almost constant by increasing the tempering temperature from 400°C to 500°C. Moreover, weight loss of all the tested samples increased almost linearly as the applied load increased since an increase in the load might increase the contact stress leading to further damage.

***Keywords*:** Ductile Iron, Dual Matrix Structure, Intercritical Austenitizing Temperature, Wear

Chapter 1

Introduction

Introduction

1.1 Motivation and Background of the present investigation

"Cast Iron is brittle" is an obsolete but broadly held truism which erroneously implies that all cast irons are the same, and none are ductile. In fact, ductile iron is a particular type of cast iron which is ductile. It offers the design engineer a unique blend of an extensive variety of high strength, wear resistance, fatigue resistance, toughness and ductility notwithstanding the remarkable advantages of cast iron such as- castability, machinability, damping properties and economy of production. Tragically, these positive characteristics of ductile cast iron are not as generally known as the mistaken impression of brittleness is well known.

Over sixty years ago, the birth of a new engineering material, ductile cast iron, was announced at the 1948 American Foundry men's Society Annual Conference and this gave a new lease on life to the cast iron family. The history of the first four decades of cast iron is the history of classical pattern of the research, development and commercialization of a new material. As knowledge of the properties and economies of ductile cast iron spread, its usage increased dramatically and it was the beginning of over 50 years of continual growth worldwide, in spite of recessions and changes in materials technology. [1-2]. The continual growth of world production of Ductile Cast Iron is shown in Figure 1.1.

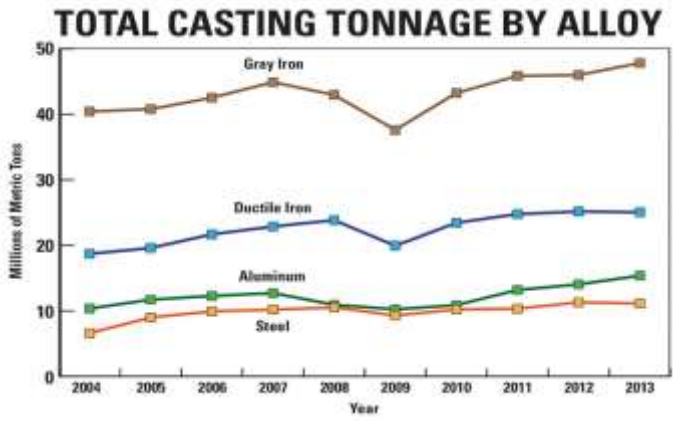

Figure: 1.1 Modern casting census of world casting production [3]

Ductile cast iron is a family of versatile cast irons exhibiting extensive variety of properties which are obtained through microstructure control. The ease with which ductile cast iron can be processed and cast into complex shapes is very much dependent on high carbon content. During solidification most of the carbon forms as graphite spheroids which exerts only a minor influence on the mechanical properties in contrast to the effect of flake graphite in grey cast iron. The matrix structure then has the greatest impact on the properties of iron. The most important and distinguishing microstructural feature of all ductile cast irons is the presence of graphite nodules which act as "crack-arresters" and give ductile cast iron ductility and toughness superior to all other cast irons, and comparable to many cast and forged steels. The final matrix structure of ductile cast iron can be advantageously altered by using a wide range of heat treatments such as normalizing, quenching and tempering, and austempering obtaining ferritic, pearlitic, martensitic and belongs to austenite-ferrite matrices. Ductile iron furnishes the designer with best blend of overall properties especially in the area of mechanical properties where it provides option of choosing high ductility, with grades guaranteeing more than 18% elongation, along with tensile strength exceeding 825 MPa. Austempered Ductile Iron (ADI) offers even better mechanical properties and wear resistance, providing tensile strengths surpassing 1600 MPa. In addition to the cost advantages offered by all castings, ductile cast iron when compared to steel and malleable iron castings, also offers further cost savings. The automotive industry has expressed its confidence in ductile cast iron through the extensive use of this material in safety related components such as steering knuckles and brake callipers. A standout amongst critical materials applications in the world is in containers for the storage and transportation of nuclear wastes. [4-6]

Despite the fact that ductile cast iron possess a good combination of mechanical properties there is an expanding demand in automotive industries for ductile cast iron with increasing

ductility without influencing the strength of ductile cast iron. In some components e.g. suspension parts of automobiles, good toughness and high ductility are needed. These requirements can be accomplished through the advancement of ductile cast iron with dual matrix structure. Matrix structure of this type of ductile cast iron comprises of ferrite (soft phase) and martensite (hard phase). This microstructure is obtained by a special heat treatment process in which the ductile iron is subjected to an incomplete austenitization stage within the intercritical intervals followed by a fast cooling step to transform austenite into martensite. The intercritical interval is a region delimited by the upper and lower critical temperatures where ferrite, graphite and austenite coexist. The tensile and proof stress of ductile iron with dual matrix structure is much higher than pearlitic, and ferrite grades and ductility is somewhat lower than ferritic grades. The combined strength-elongation percentage of ductile iron with dual matrix structure is often referred as Developed-Austempered Ductile Iron. [7-13]

With the increasing applications of the ductile cast iron as the substitute for other cast iron and fabricated steels, the understanding of the wear behaviour of ductile cast iron is crucial. The wear studies conveyed in the past are principally leaned towards the ductile cast iron, cast iron and austempered ductile irons. However, a few attempts have so far been made in determining the wear behaviour of ductile cast iron iron with ferrite-martensite matrix by controlling the ferrite and martensite volume fractions. This study has been, accordingly, embraced to examine the influence of intercritical austenitizing temperature (ICAT), quenching media and tempering temperature on mechanical properties and wear behaviour of ductile iron with dual matrix structure (DMS). [14-19]

1.3 Objective of the Present Work

Ductile iron with dual matrix structure having ferrite and martensite were developed by intercritical heat treatment process, and quenched and tempered ductile iron with dual matrix structure is obtained by intercritical heat treatment process followed by tempering. The objectives of the present investigation are:

1. To study the effect of intercritical austenitizing temperature and quenching media on the microstructure and mechanical properties of ductile iron with dual matrix structure.
2. To study the effect of different tempering temperatures on the microstructure and mechanical properties of quenched and tempered ductile iron with dual matrix structure.
3. To study the wear behaviour of ductile iron with dual matrix structure and quenched and tempered ductile iron with dual matrix structure under various applied loads.

……

Chapter 2
Literature Review

Literature Review

2.1 Cast Iron- A Natural Composite

Cast irons are fundamentally iron-carbon alloys having carbon in the range of 2.11% and 6.67%. Eutectic reaction takes place during solidification. Alloys having carbon less than 4.3% are called hypo-eutectic cast irons; the alloy containing 4.3%C is called eutectic cast iron; and the alloys containing more than 4.3% carbon are called hyper-eutectic cast irons. The castibility is best of an eutectic alloy. The industrial cast iron has carbon normally in the range of 2.11% to 4%, alongside components elements like silicon, manganese, sulphur and phosphorus in substantial amounts. Higher carbon content makes them more brittle. The ductility of cast iron is very low, and it cannot be forged, rolled, drawn etc. at room temperature but can be cast into desired shape and size by pouring the molten alloy of desired composition into a mould of desired shape and allowing it to solidify. As casting is the only and exclusively suitable process to shape these alloys, so called cast iron. The principle of cast iron solidification is understood from the Iron-Carbon-Silicon (2%) ternary phase diagram as shown in the Figure 2.1. [20, 21]

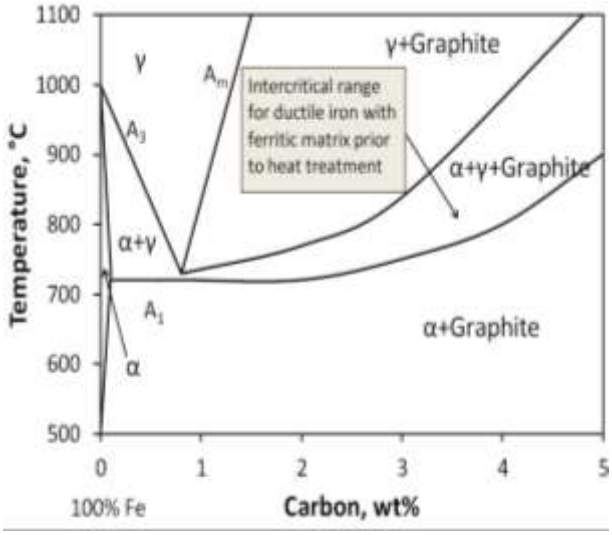

Figure: 2.1 Iron-Carbon-Silicon (2%) ternary phase diagram

Cast irons are natural composite, by proper alloying, good foundry control, and appropriate heat treatment; the properties of any type of cast iron may be fluctuated over an extensive range of applications. There are four variables to be considered which prompts to the different types of cast iron, namely the carbon content, the alloy and impurity content, the cooling rate during and after freezing, and the heat treatment after casting. These variables control the condition of the carbon and also its physical form. Cast iron can be cast all the more effortlessly then steels. The grey cast iron has good casting properties, good vibration damping, good wear resistance, good machinability and low notch sensitivity. However, its tensile strength and elongation are very low, so it can only produce some metal parts with low physical requirements, such as protective cover, cover, oil pan, hand wheels, frame, hammer, small handle, base, frame, box, knife, bearing seat, wheels, cover, pump, valve, pipe, flywheel, motor blocks etc. As for the higher grades, grey cast iron can withstand greater load and a certain degree of tightness or corrosion resistance of the more important castings such as cylinder, gear, flywheels, cylinder block, cylinder liner, piston, gear box, brake wheel, coupling plate, medium pressure valve, etc. Ductile cast iron has engineering properties similar to steel, and near-net shaped castings are replacing forgings, weldments, and steel castings in a variety of applications. Ductile cast iron is likewise accessible in continuously cast bar stock and can be a direct replacement for carbon steel bars in a number of gears in the automotive, hydraulic, machine tool, and other industries. [22-23]

2.2 History of Ductile Cast Iron

The scientists were looking for cast iron having mechanical properties comparable with steel. In their endeavour produce a cast iron better than the malleable iron, in 1943, at the International Nickel Company Research Laboratory, Keith Dwight Millis made a ladle addition of Magnesium to cast iron; the solidified castings contained not flakes, but nearly perfect spheres of graphite. Five years later, at the 1948 AFC Convention, Henton Morrogh

of the British Cast Iron Research Association announced the successful production of spherical graphite in hypereutectic grey iron by the addition of small amounts of cerium. At the time of Morrogh's presentation, the International Nickel Company revealed their development starting with Millis' discovery in 1943, of magnesium as a graphite spherodizer. On October 25, 1949, patent 2,486,760 was concede to the International Nickel Company, assigned to Keith D Millis, Albert P. Gegnebin and Norman B. Pilling. This was the official birth of ductile cast iron.

(a) (b)

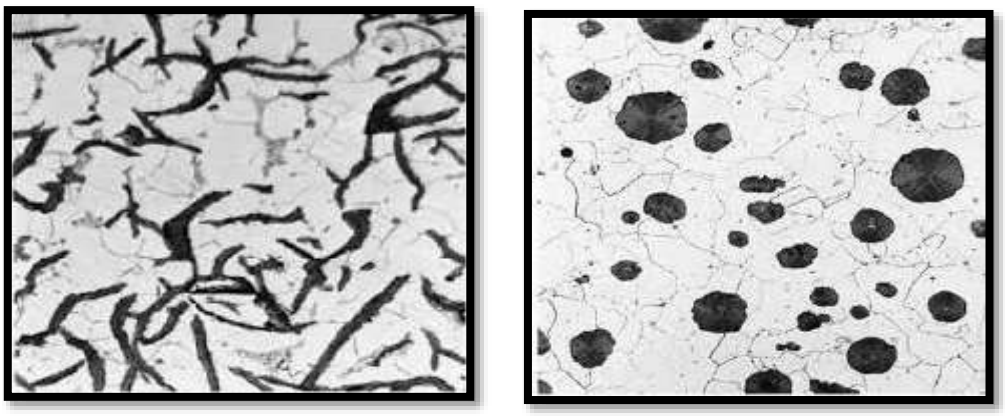

Figure: 2.2 Microstructure of (a) Grey Cast Iron and (b) Ductile Cast Iron

Ductile Cast Iron also known as Nodular Iron, Spheroidal Graphite Iron and Spherulitic Iron is a cast iron in which the graphite is in the form of nodules rather than flakes as it is in the grey cast iron. The compact spheroids interrupt the continuity of the matrix much less than graphite flakes, and also inhibit the creation of cracks, these outcomes enhanced ductility compared with a similar structure of grey cast iron and that gives the alloy its name. The formation of nodules is achieved by the addition of nodulizing elements, most commonly magnesium and, less often now, cerium. Tellurium has also been used. Yttrium, often a component mischmetal has also been used as possible nodulizer. The matrix phase surrounding these particles is either pearlite or ferrite, depending on heat treatment as shown in the Figure 2.2 (b). Castings are stronger and much more ductile than grey iron, as a

comparison of their mechanical properties. In fact, ductile cast iron mechanical characteristics are comparable with those of steel. For example ferritic ductile irons have tensile strength ranging between 380 and 480 MPa and ductilities from 10% to 20 % (as percentage elongation). [4, 20, 24]

2.2.1 Family of Ductile Cast Iron

Ductile cast iron is not a single material, but a family of materials offering a wide range of properties obtained through microstructure control. The common feature that all ductile cast irons share is the spherical shape of the graphite nodules. With a high percentage of graphite nodules present in the structure, mechanical properties are determined by the ductile cast iron matrix. The importance of matrix in controlling mechanical properties is emphasized by the use of matrix names to designate the following types of ductile iron.

1. Ferritic Ductile Iron- Graphite spheroids in a matrix of ferrite provide an iron with good ductility and impact resistance and with a tensile and yield strength equivalent to low carbon steel. Ferritic ductile iron can be produced "as-cast" but may be given an annealing heat treatment to assure maximum ductility and low temperature toughness.

2. Ferrito- Pearlitic Ductile Iron- These are the most common grade of ductile cast iron and are normally produced in the "as cast" condition. The graphite spheroids are in a matrix containing both ferrite and pearlite. Properties are intermediate between ferritic and pearlitic grades, with good machinability and low production costs.

3. Pearlitic Ductile Iron- Graphite spheroids are embedded in a matrix of pearlite resulting in an iron with high strength, good wear resistance, and moderate ductility and impact resistance. Machinability is also superior to steels of comparable physical properties.

4. Martensitic Ductile Iron- Using sufficient alloy additions to prevent pearlite formation, and a quench-and-temper heat treatment produces this type of ductile cast iron. The resultant

tempered martensite matrix develops very high strength and wear resistance but with lower levels of ductility and toughness.

5. Austenitic Ductile Iron- Alloyed to produce an austenitic matrix, this ductile cast iron offers good corrosion and oxidation resistance, good magnetic properties, and good strength and dimensional stability at elevated temperatures.

6. Austempered Ductile Iron (ADI) **-** ADI, the most recent addition to the ductile iron family, is a sub-group of ductile irons produced by giving conventional ductile iron a special austempering heat treatment. Nearly twice as strong as pearlitic ductile iron, ADI still retains high elongation and toughness. This combination provides a material with superior wear resistance and fatigue strength.

2.2.2 Properties of Ductile Cast Iron

Matrix control, obtained in conventional ductile cast iron either "as-cast" through a combination of composition and process control, or through heat treatment, gives the designer the option of selecting the grade of ductile iron which provides the most suitable combination of properties. With ductile iron, the safety and reliability of process equipment is improved. The improved mechanical properties increase its resistance to breakage from physical load, or mechanical and thermal shock far above that of grey iron. The corrosion resistance of ductile cast iron is equal or superior to cast steel in many corrosive atmospheres. Its wear resistance is comparable to some of the best grades of steel and superior to grey cast iron in heavy load or impact load situations. Because it can be cast with the same low cost procedures used for grey cast iron it is considerably less expensive than cast steel and only slightly more expensive than grey cast iron. The substantial advantages obtained from its high yield strength and ductility make it an economical choice for many applications [25, 26]. Table 2.1 compares the mechanical properties of ductile cast iron with cast iron, malleable iron and cast steel.

Table: 2.1 Mechanical properties of Ductile Cast Iron compared with Cast Iron, Malleable Iron, and Cast Steel

Materials → **Mechanical properties ↓**	**Ductile Cast Iron ASTM A395**	**Cast Iron ASTM A48 Class 25**	**Malleable ASTM A47Grade 32510**	**Cast Steel ASTM 216Grade WCB**
Tensile Strength, MPa	**413**	**172**	**345**	**483**
Yield Strength, MPa	**276**	**_**	**224**	**248**
Elongation %	**18%**	**_**	**10%**	**22%**

The strong influence of matrix structure on different tensile properties of ductile cast iron produces significant correlations between these properties. Figure 2.3 illustrates the non-linear least square relationships between tensile and yield strengths and the dynamic elastic modulus. In 1970 Siefer and Orths, in a statistical study of the properties of a large number of ductile cast iron samples, identified a relationship between tensile strength and elongation of the form

$$(\text{Tensile strength})^2 \times (\text{elongation \%}) \div 1000 = Q; \text{ where Q is a constant}$$

A large value of Q indicates a combination of higher strength and elongation and therefore, higher material performance.

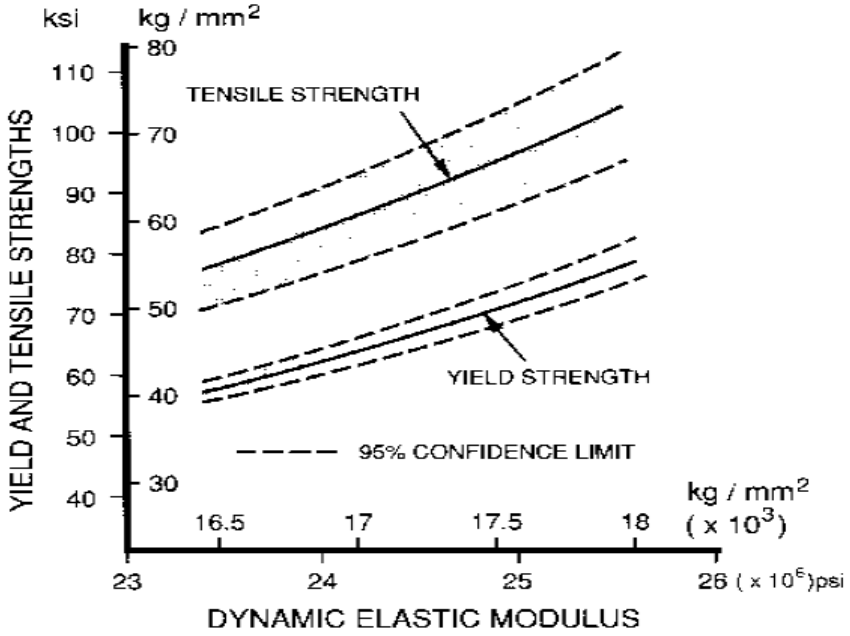

Figure: 2.3 Relationships between yield and tensile strengths and dynamic elastic modulus for ductile cast iron.

2.2.3 Advantages of Ductile Cast Iron

The advantages of ductile cast iron which have led to its success are numerous, but they can be summarized as - versatility and higher performance at lower cost. As illustrated in Table:2.1 other members of the ferrous casting family may have individual properties which might make them the material of choice in some applications, but none have the versatility of ductile cast iron, which often provides the designer with the best combination of overall properties. This versatility is especially evident in the area of mechanical properties where ductile cast iron offers the designer the option of choosing high ductility, with grades guaranteeing more than 18% elongation, or high strength, with tensile strengths exceeding 825 MPa. Austempered Ductile Iron (ADI) offers even better mechanical properties and wear resistance, providing tensile strengths exceeding 1600 MPa.

In addition to the cost advantages offered by all castings, ductile cast iron, when compared to steel and malleable iron castings, also offers further cost savings. Like most commercial cast metals, steel and malleable iron decrease in volume during solidification, and as a result,

require attached reservoirs (feeders or risers) of liquid metal to offset the shrinkage and prevent the formation of internal or external shrinkage defects. The formation of graphite during solidification causes an internal expansion of ductile cast iron as it solidifies and as a result, it may be cast free of significant shrinkage defects either with feeders that are much smaller than those used for malleable iron and steel or, in the case of large castings produced in rigid moulds, without the use of feeders. The reduction or elimination of feeders can only be obtained in correctly designed castings. This reduced requirement for feed metal increases the productivity of ductile cast iron and reduces its material and energy requirements, resulting in substantial cost savings. The use of the most common grades of ductile cast iron "as-cast" eliminates heat treatment costs, offering a further advantage. [27]

2.3 Ductile Iron with Dual Matrix Structure

Ductile Iron (DI) with Dual Matrix Structure (DMS) is a new class of materials that in the early 80's was first introduced as Soft Eye and Hard Eye. Matrix structure of this type of DI consists of ferrite (soft phase) and martensite or banite (hard phase) that are formed by a special heat treatment process. The DI with DMS having ferrite-martensite structure is obtained by intercritically austenitizing the DI in two phase region ($\alpha + \gamma$) followed by rapid cooling to transform austenite into martensite. The intercritical heat treatment has an advantage of precise control of ferrite and martensite volume fractions [7, 8]

In some components, e.g. suspension parts of automobiles, good toughness and high ductility are required. These necessities are met by this newly developed DI with DMS that shows tensile and proof strengths, together with hardness, similar to pearlitic grades, but ductility at the same level of ferritic irons. Recently it has been shown that the tensile and proof stresses of DI with DMS are much higher than pearlitic and ferritic grades and ductility is marginally lower than ferritic grades. It has been shown that the tensile strength and ductility can

agreeably be optimized by critical combinations of austenitizing and tempering time and martensite volume fraction. [28-30]

2.3.1 Intercritical Austenitizing Temperature (ICAT)

Intercritical heat treatments in ductile cast iron start with partially austenitizing the material at the intercritical temperature range. The ICAT of the heat treatment plays a major role in the final microstructure of the material and therefore the mechanical properties. For a given alloy chemistry, the volume fraction of austenite is determined by the ICAT. It can be deduced from the vertical section of iron-carbon-silicon ternary diagram at 2% Si using the lever rule that increasing the ICAT increases the amount of austenite and decreases the amount of ferrite. Therefore, the ICAT step determines the amount of austenite transformation products in the final microstructure. Also, it has been reported that at the ICAT the austenite starts to nucleate at the eutectic cells and the intercellular boundaries, which are considered the preferential sites for heterogeneous nucleation. The carbon content of the high temperature austenite is determined by the ICAT. Studies performed in unalloyed ductile iron with ferritic matrices prior to heat treatment have shown that the carbon to form the austenite at high temperatures comes from the graphite nodules; and, therefore, the carbon concentration in the austenite increases as the ICAT increases. [11, 12, 31-34]

Some authors have used ductile iron with ferritic-pearlitic matrices as starting microstructures. Under these conditions the carbon to form the austenite at high temperature comes from the carbon in the pearlite and the diffusion of carbon from the graphite nodules is limited. When the pearlite completely dissolved the graphite nodules start providing carbon to reach the equilibrium austenite volume fraction and carbon concentration. [35-37]

2.3.2 Ferrite to Austenite Transformation

In case of a homogenous chemical distribution, austenite is preferably nucleated on carbides on ferrite-ferrite grain boundaries and triple points, rather than at carbides inside ferrite grains, shown in Figure 2.4. It is most likely that carbides at grain boundaries are more energetically favourable sites for nucleation than isolated carbides inside ferrite grains. The solubility of carbon in ferrite is low but the diffusion rate in ferrite is much higher than in austenite. Carbon from the dissolving carbides thus diffuses through the ferrite via bulk diffusion or via ferrite grain boundaries to the growing austenite areas. [38]

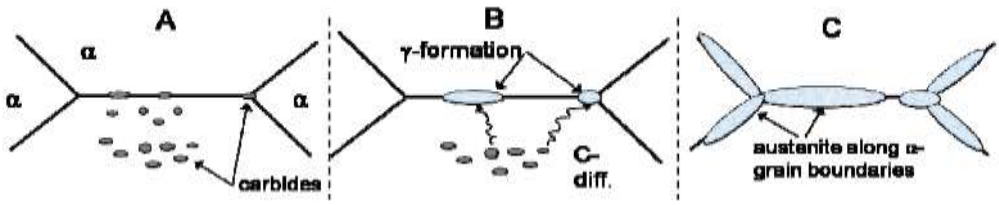

Figure 2.4 Schematic picture of austenite (γ) formation on ferrite-ferrite (α) grain boundaries and triple points**.**

In Figure 2.5 is an example of the length change, or dilatation during heating and cooling is presented. When heated the material expands thermally which is visible as a linear increase in volume or length of the sample. When the Ac_1- temperature is crossed during heating the ferrite to austenite (α→γ) transformation starts. Since the specific volume of austenite is smaller than the one for ferrite, the α→γ transformation results in a volume decrease. When the austenization is complete, at A_{C3} the thermal expansion of the austenite yields an increase in dilatation, visible as a nail on the dilatation curve

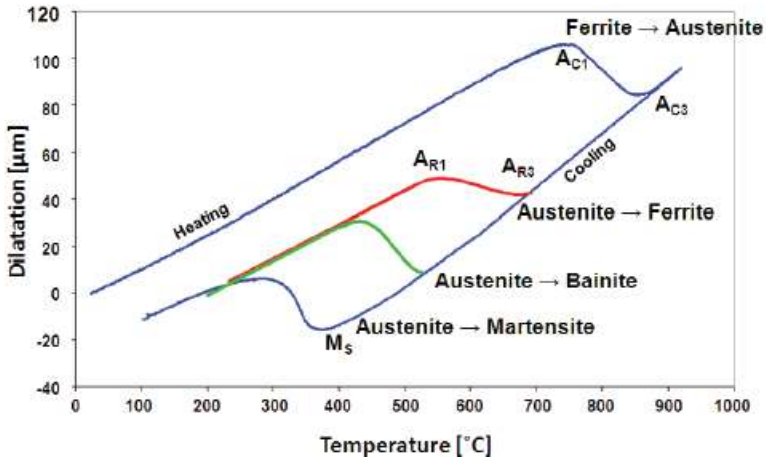

Figure 2.5 Schematic dilatation curve(s) indicating structural changes during heating and cooling in a dilatometer

There is no available data in the literature about the segregation of substitutional elements in ductile cast iron during intercritical austenitizing. However, studies performed in DP steels suggest that the partitioning of elements such as silicon, nickel and manganese during intercritical austenitizing may be limited due to the low rate of substitutional diffusion at the temperatures of the heat treatment. As a result, the concentration of those elements in the austenite is determined mainly by the chemistry of the alloy and their segregation during the solidification process. Therefore, austenite particles formed at the eutectic cells are expected to have a higher manganese concentration. While austenite particles formed near the graphite nodules will have a higher concentration of nickel, silicon and copper. [39-41]

2.4 Cooling and Quenching media

After intercritical austenitizing, the material can be fast cooled to a temperature below the martensite start temperature (quenching), transforming the high temperature austenite to martensite. Intercritical austenitizing followed by quenching is used to produce DI with DMS. The microstructure of DI with DMS consists of a continuous matrix of ferrite plus particles of martensite. The ferrite matrix provides good ductility and the martensite particles act as the strengthening phase.

The quenching media and the degree of agitation in the quench bath are essential variables that can be used to ensure that a suitable microstructure is produced by the quenching process. Agitation of the quenching bath may be obliged to increase both quench severity and the uniformity of cooling in complex castings or batches of castings. To minimize internal stresses, distortion and cracking, especially in complex castings, the least severe quenching media that produces the desired microstructure ought to be chosen. As the required severity of quenching increases, it becomes increasingly important to temper the castings immediately after quenching. Common quench media are discussed underneath [20, 42- 43].

Water: Water is genuinely good quenching media. It is cheap, accessible, easily stored non-toxic, non-flammable smokeless and simple to filler and pump yet with water quench the formation of bubbles may bring about soft spots in the metal. Agitation is recommended with use of water quench. Still other issues with water quench included its oxidizing nature, its corrosivity and the tendency to excessive distortion and cracking.

Salt Water: Salt water is a severe rapid quench media than plain water because the bubbles are broken easily and allow for rapid cooling of the part. However, salt water is even more corrosive than plain water, and consequently must be flushed off instantly..

Oil: Oil is used when a slower cooling rate is wanted. Since oil has a very high boiling point, the transition from start of martensite formation to the finish is slow and this lessens the probability of cracking. Oil quenching results in fumes, spills, and at times a fire hazard.

Polymer quench: Polymer quenches that will produce a cooling rate in between water and oil. The cooling rate can be adjusted by varying the components in the mixture-as these are composed of water and some glycol polymers. Polymer quenching is capable of producing repeatable results with less corrosion than water and to a lesser extent a fire hazard than oil.

However, these repeatable results are conceivable only with constant monitoring of the chemistry.

Cryogenic Quench: Cryogenics or deep freezing is done to verify there is no retained austenite during quenching. The amount of martensite formed at quenching is a function of the lowest temperature encountered. At any given temperature of quenching there is a certain amount of martensite and the balance is untransformed austenite. This untransformed austenite is very brittle and can cause loss of strength or hardness, dimensional instability, or cracking.

2.4.1 Epitaxial Ferrite Formation

The formation of new ferrite by transformation of austenite by epitaxial growth on retained ferrite (ferrite present during ICAT) during cooling from ICAT is called epitaxial ferrite. The extent of retransformation of austenite to epitaxial ferrite is a consequence of the stability of the austenite; i.e. the amount and type of the austenite stabilizing elements. Carbon is an austenite stabilizing elements. However, diffusivity of carbon compared to the diffusivity of substitutional solutes like Mn and Si is high and sufficient amounts of Mn and or Si are thus required to withstand massive formation to epitaxial ferrite. [44-45]

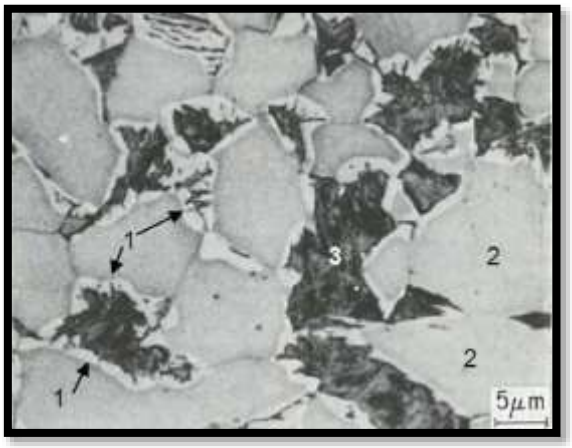

Figure 2.6 Formation of epitaxial ferrite rim around austenite particles in 0.6C-1.5Mn-0.05Nb steel. 1=epitaxial ferrite (white), 2=retained ferrite (gray), 3= martensite (black) [46].

Slow cooling epitaxial ferrite formed preferentially on the pre-existing ferrite within the austenite pools. Then again, on faster cooling they found that the growth of the epitaxial ferrite took place specially around the edge of the austenite particles. The combination of large deriving force is needed for the austenite to epitaxial ferrite transformation at rapid cooling rate and a large ferrite–austenite interfacial area encompassing the austenite adds to the envelopment of the martensite phase with a ring of epitaxial ferrite The formation of epitaxial ferrite brings about an enrichment of carbon in the remaining austenite – which consequently yields a lower carbon content in the new ferrite – which in turn makes the austenite more stable and thus lowers the martensite start(M_S) temperature. [44-47]

2.4.2 Martensite Formation

The austenite to martensite transformation is normally considered to be an athermal diffusionless transformation, occurring when the austenite is cooled underneath the M_S temperature. The martensite thus has the same chemical composition as its parent austenite. Since martensite formation is diffusionless the carbon atoms will be trapped in the octahedral sites of a bcc structure. The solubility of carbon is significantly surpassed and martensite assumes a body-centered tetragonal unit cell, bct, at adequately high carbon content. The volume increase that follows an austenite → martensite transformation is obviously visible in a dilatation curve, Figure 2.5.

Martensite formation includes a shape change which infers that plastic deformation of the austenite must accompany the development of a martensite crystal. Alternately, the surrounding ferrite phase must experience a plastic deformation in order to accommodate the shape change and the volume increase that follows martensite formation. It is observed experimentally that the dislocation density in the ferrite increments with the amount of martensite formed.

Since the martensite phase is a phase supersaturated with carbon, it is not a steady phase. If the structure is heated to temperatures where carbon atoms are mobile, the carbon will diffuse from the octahedral sites and form carbides.

The temperature for martensite start formation, (M_S) reflects the amount of thermodynamic driving force needed to initiate the transformation of austenite to martensite. M_S is highly dependent on the chemical composition of the austenite and can be calculated using different empirical relationships. One commonly used is the Steven-Haynes (SH) relationship

$$M_S = 561 - 474C - 33Mn - 17Cr - 17Ni - 21Mo \quad (1)$$

From equation (1) it is clear that M_S decreases essentially with increasing carbon content. The carbon content of the austenite is a consequence of the temperature from which quenching takes place [48-50].

2.5 Quenched and Tempered Ductile Iron with Dual Matrix Structure

Quenched and tempered ductile iron with dual matrix structure is obtained by intercritical austenitizing followed by quenching and tempering, which provides a microstructure of graphite nodules in a matrix of ferrite plus tempered martensite particles. The matrix of the iron resembles the microstructure of dual phase steels. Tempering consists of heating the material below the eutectoid temperature which leads to the decomposition of the untempered martensite into ferrite plus iron carbides precipitates. The objectives of this process include reducing the brittleness of quenched materials, improvement of toughness and ductility, and also, reducing the probability of cracking. Reheating the DMS ductile iron involves different mechanisms dependent on which phase is the subject; the ferrite phase will undergo an over ageing process and the martensite will be tempered. The strength depends strongly on the volume fraction of martensite in the microstructure, while the elongation is mainly related to the tempering conditions.

Research has been performed in order to elucidate the role of tempering conditions and martensite volume percent and morphology on the mechanical properties of quenched and tempered ductile iron with dual matrix structure. However, there is less available report on the effect of tempering variables on mechanical properties of DI with DMS. The only considerable report belongs to Okabayashi et al. whose results indicate that impact strength of the samples, tempered at 600°C for 20 min, is better than those tempered at 200°C for 1 hour. According to Kobayashi and Yamoto the combined strength-elongation percentage of DMS ductile cast iron with ferrite–bainite matrix that is often referred to as Developed-ADI, is better than the conventional austempered ductile cast iron. The results of the work carried out by Wade et al. indicated that the mechanical properties of DMS ductile cast iron with a ferrite–bainite matrix are improved, more than those of the same DMS cast iron with a ferrite–martensite matrix. [28, 29, 51-55]

Rashidi et al. studied the effect of tempering conditions (tempering temperature and tempering time) on the mechanical properties of DMS ductile cast iron [8]. The author demonstrated that within the tempering temperature range of 400-500°C, impact strength and elongation suddenly increases, whereas within the same temperature range, the ultimate tensile strength and yield strength remain almost constant. By increasing the tempering temperature, except for the tempering temperature range of 400°C –500°C, both tensile and yield strength decrease. Longer duration of tempering period at 500°C increases the elongation percentage for tempering period up to 120 minutes followed by a gradual decrease. The effects of tempering temperature on the yield stress, ultimate tensile strength, impact strength and elongation percentage are demonstrated in Figure 2.7 and the effect of tempering time when the temperature is 500°C is shown in Figure 2.8 [8].

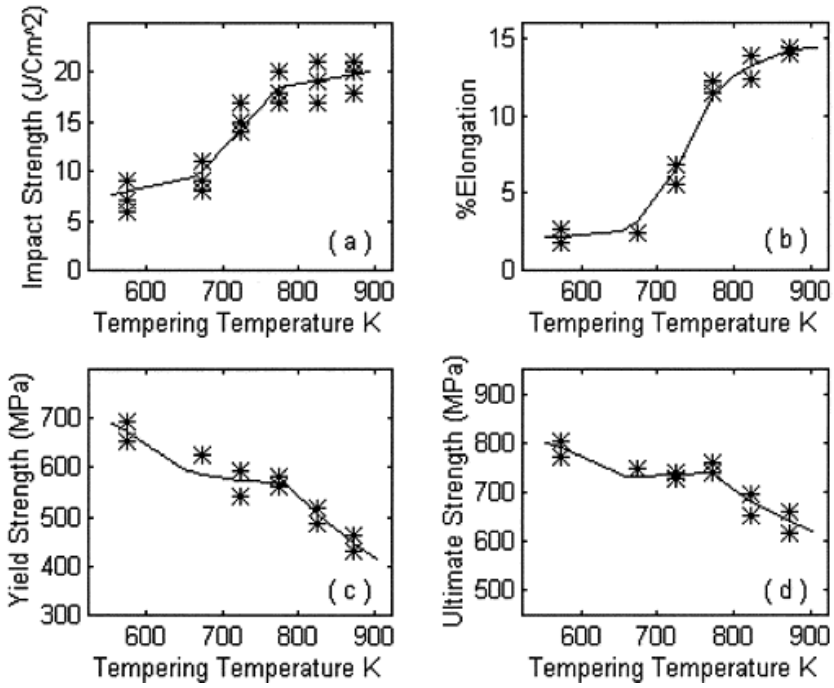

Figure: 2.7 Effect of tempering temperature on: (a) Impact strength, (b) Elongation %, (c) Yield strength, and (d) Tensile strength [8].

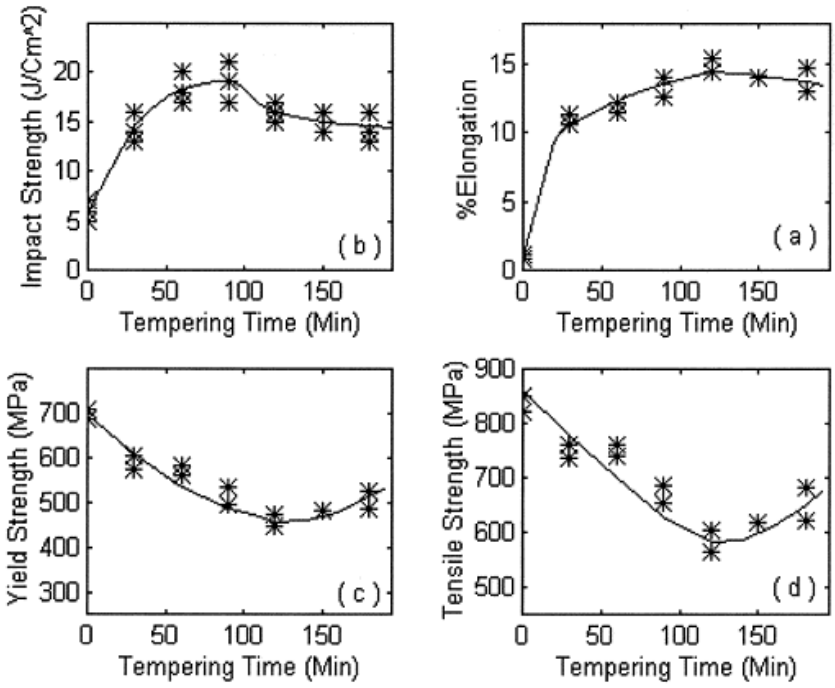

Figure: 2.8 Effect of tempering time at constant tempering temperature at 500°C on a) Elongation %, (b) Impact strength, (c) Yield strength, and (d) Tensile strength [8].

Sayed et al studied the effect of tempering temperature on microstructure and mechanical properties of dual phase steels. The material was intercritically annealed at 760°C and quenched in water and then tempered at within the range of 100°C -600°C. The results indicated that after tempering at 200°C the yield strength increases slightly and ultimate tensile strength remains unchanged and on further increase in tempering temperature both yield strength and ultimate tensile strength decreases [56].

2.6 Wear

The nature of most metal products relies on upon the states of their surfaces and on the surface deterioration due to use. Surface deterioration is critical in engineering practice, as it often confine the life and performance of the machining components. Wear is an accidental deterioration resulting from use or environment. Wear is related to interactions between surfaces and specifically the removal and deformation of material on a surface as an after effect of mechanical action of the opposite surface. The need for relative motion between two surfaces and initial mechanical contact between asperities is a vital distinction between mechanical wear contrasted to other processes with similar outcomes. Wear is fundamentally a surface phenomenon and one of the most destructive influences to which metals are exposed. The displacement and detachment of metallic particles from a metallic surface may be brought about by contact with (a) another metal (adhesive metallic wear), (b) a metallic or a non-metallic abrasive, or (c) moving liquids or gases (erosion).

2.6.1 Wear mechanism

Some commonly referred wear mechanism includes:

1. Adhesive wear: Adhesive wear, can be found between surfaces amid frictional contact and by and large alludes to unwanted displacement and attachment of wear debris and material compounds from one surface then onto the next. Adhesive wear are caused by relative

motion, "direct contact" and plastic deformation which create wear debris and material transfer from one surface to another.

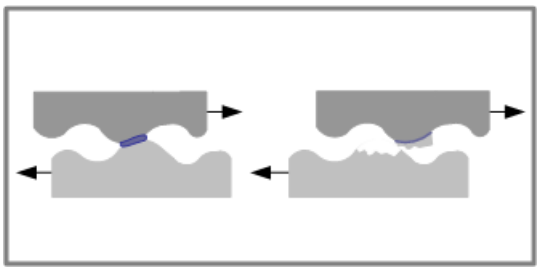

Figure 2.9(a) Schematic representations of the adhesive wear mechanism

2. Abrasive wear: Abrasive wear happens when hard particles slide or roll under pressure across a surface or when a hard surface rubs across another surface. The abrading particles from the harder object have a tendency to scratch or gouge the softer material.. The simplicity with which the deformed metal may be torn off depends upon the toughness.

Abrasive wear is usually classified by sort of contact and the contact environment. The type of contact determines the mode of abrasive wear. The two modes of abrasive wear are known as two-body and three-body abrasive wear. Two-body wear occurs when the grits or hard particles remove material from the opposite surface. Three-body wear occurs when the particles are not constrained, and are free to roll and slide down a surface.

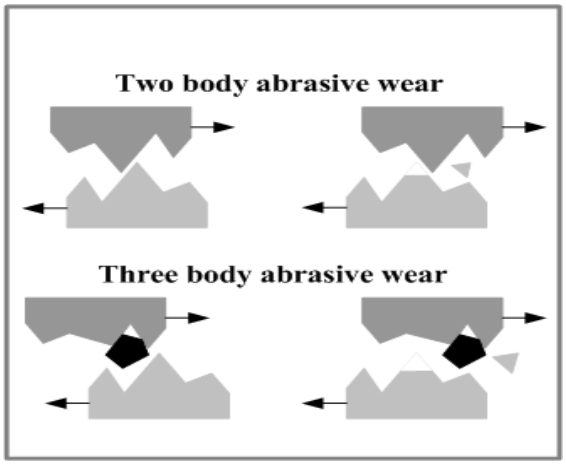

Figure 2.9(b) Schematic representations of the abrasive wear mechanism

3. Fatigue wear: Fatigue wear of a material is brought about by cyclic loading during friction. Fatigue occurs if the applied load is higher than the fatigue strength of the material. Fatigue cracks begins at the material surface and spread to the subsurface regions. The cracks may connect to each other resulting in separation and delamination of the material pieces.

One of the types of fatigue wear is **fretting wear** caused by cycling sliding of two surfaces across each other with small amplitude (oscillating). The friction force produces alternating compression-tension stresses, which result in surface fatigue.

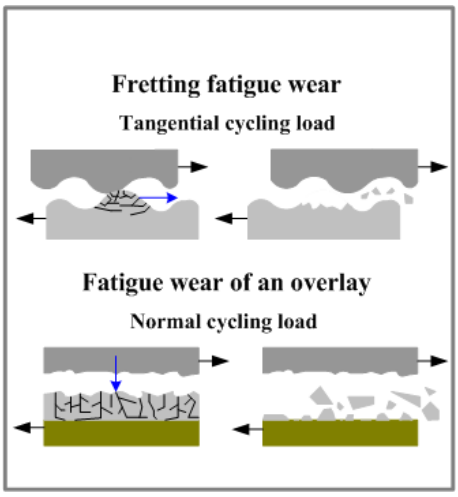

Figure 2.9(c) Schematic representations of the fatigue wear mechanism

4. Erosive Wear: Erosive wear can be defined as the process of metal removal due to impingement of solid particles on a surface. Erosion is caused by a gas or a liquid, which may or may not carry entrained solid particles impinging on a surface. When the angle of impact is small, the wear produced is closely analogous to abrasion. When the angle of impact is normal to the surface, material is displaced by plastic flow or is dislodged by brittle failure.

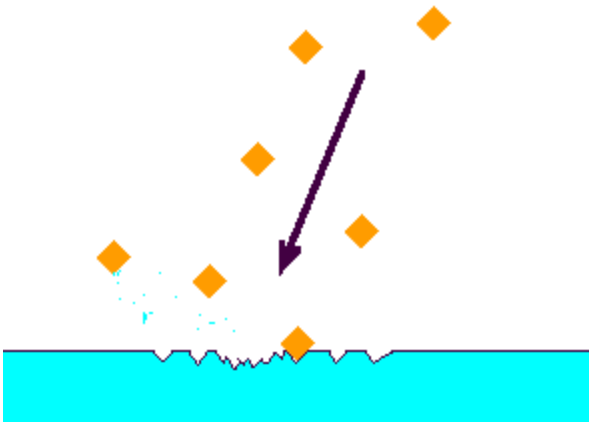

Figure 2.9(d): Schematic representations of the erosive wear mechanism

2.6.2 Recent trends in ductile cast iron wear research

With the increasing applications of the DI as a substitute for other cast iron and fabricated steels, the understanding of the wear behaviour of DI is crucial. Wear properties is not an intrinsic property of a material but depends upon the properties of the micro-constituents of the materials, test condition and environment [57-59].

Recently, several attempts have been made to study the wear behaviour of different class of DI. For example, Islam et al. studied the wear behaviour of as-cast and heat treated DI under dry sliding condition. The results show that the wear mechanism is mainly adhesive wear for heat treated samples and a combination of delamination and adhesive wear for as-cast samples, this difference in wear behaviour lies in the matrix structure of the DI [17].

Zimba et al. investigated the wear resistance of Austempered Ductile Iron (ADI). It was concluded that wear resistance of ADI is much superior to that of the parent DI and almost same to that of steel whose hardness is approximately twice that of ADI [60].

Sahin et al. studied the wear behaviour of ADI with DMS. The ductile iron sample was intercritically austenitized at various temperatures of 795°C and 815°C for 20 minutes and quenched into salt bath held at austempering temperature of 365°C for various time to obtain

ADI with different ausferrite volume fractions distributed in ferrite region. The experimental result shows that increasing the austempering time caused more ductile ausferritic structure to displace hard martensite. In all austempered samples the abrasive weight loss increased with increasing austempering time [61].

Sahin et al. reports the effects of Martensite Volume Fraction (MVF) and tempering time on the abrasive wear of ferrite DI with DMS. The conclusion drawn was that the wear of the tested samples increased approximately linearly with the increasing applied load and decreasing MVF [59].

Movahed et al. investigated the tensile properties and work hardening behavior of dual phase (ferrite-martensite) steels. It was reported that dual phase steels with equal amount of ferrite and martensite shows excellent mechanical properties [62].

Aprameyan et al. studied the wear behavior of ferrite-martensite dual phase steel at four different intercritical temperatures of 730°C, 750°C, 780°C and 810°C. The result reveals that the amount of martensite volume fraction in the dual phase microstructure increases with the increases in intercritical temperature and wear resistance of dual phase steel increases with the increase in percentage volume fraction of martensite in dual phase ferrite-martensite microstructure [63].

The wear studies carried out in the past are mainly leaned towards the DI, ADI's and steels. However, a few attempts have so far been made in determining the wear behavior of DI with ferrite-martensite matrix by controlling the ferrite and martensite volume fraction and tempering temperatures. This study has been therefore, undertaken to investigate the influence of ICAT, quenching medium and tempering temperature on mechanical properties and wear behavior of DI with DMS and quenched and tempered DI with DMS.

……

Chapter 3

Experimental Details

Experimental Details

This chapter portrays the experimental procedure as adopted in the present investigation. The equipment/instruments used to carry out the experiments are listed below indicating their specific use in the project along with their specifications and particulars in details. A detailed report is also provided on the heat treatment that has been carried out to produce DI with DMS and quenched and tempered DMS samples. The following work plan has been adopted:

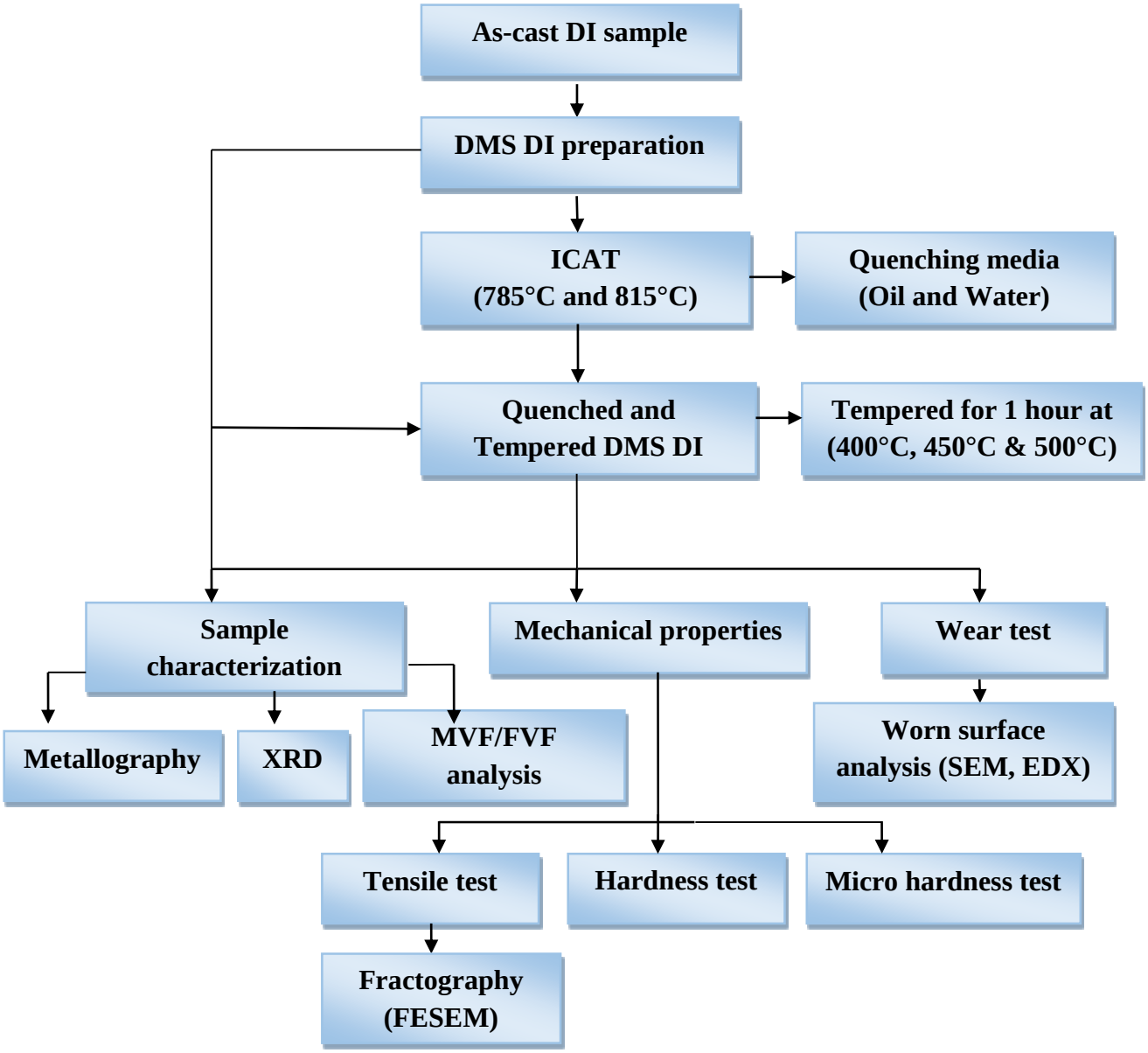

Figure 3.1 Work Plan for present investigation

3.1 Test sample preparation

The chemical composition of the as-cast DI is given in Table 3.1. The DI was produced in a medium frequency induction furnace in a commercial foundry (L&T Kansbahal, India).

Table: 3.1 Chemical composition of employed ductile cast iron

Elements	**C**	**Si**	**Mn**	**S**	**P**	**Cr**	**Ni**	**Mo**	**Cu**	**Mg**	**Ce**	**Fe**
Weight%	**3.56**	**2.07**	**0.17**	**0.009**	**0.018**	**0.03**	**0.44**	**0.001**	**0.009**	**0.041**	**0.003**	**Rest**

3.2 Heat Treatment

After fabrication the test specimens were intercritically austenitized in two phase region (α+γ) at the intercritical temperature range followed by quenching process. For the experiment, the specimens were intercritically austenitized at temperatures of 785°C and 815°C and two quenching media paraffin liquid light oil and water were selected for a detailed study of the development of DMS with different ferrite and martensite volume fraction and microstructural refinement. The quenched samples were tempered at various tempering temperature of 400 °C, 450°C and 500°C for 1 hour to obtain quenched and tempered ductile iron with dual matrix structure.

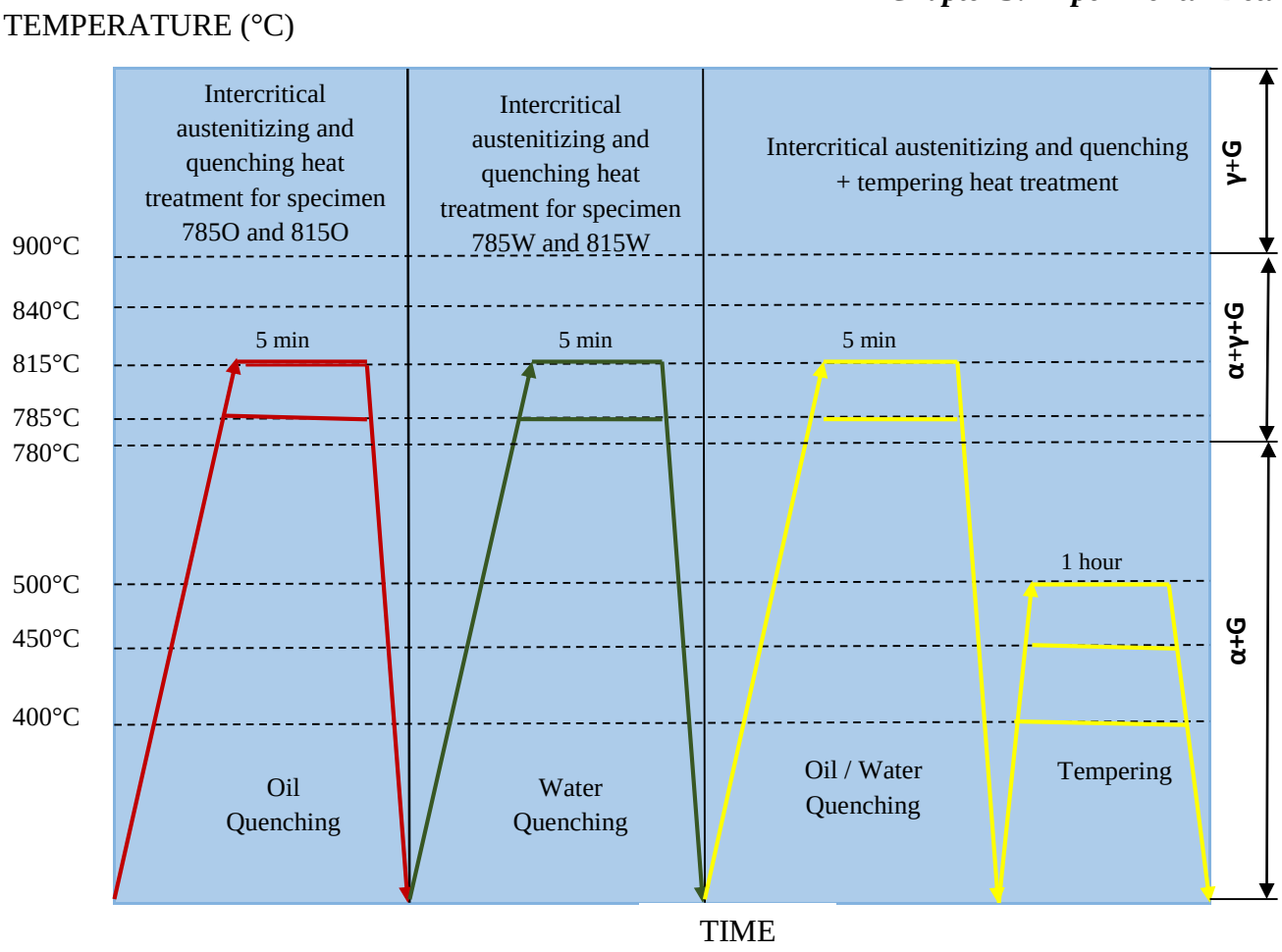

Figure 3.2 Summary of heat treatment

The specimen was coded according to different intercritically austenitized temperatures, quenching medium and tempering temperatures. The specimen code are described as such

Table: 3.2 Description of specimen code used in present work.

Specimen Code	Intercritical austenitizng temperature (ICAT)	Quenching medium	Tempering temperature
A785O	785°C	Oil quenched	-
A815O	815°C	Oil quenched	-
A785W	785°C	Water quenched	-
A815W	815°C	Water quenched	-
A785O-T400	785°C	Oil quenched	400°C

A785O-T450	785°C	Oil quenched	450°C
A785O-T500	785°C	Oil quenched	500°C
A785W-T400	785°C	Water quenched	400°C
A785W-T450	785°C	Water quenched	450°C
A785W-T500	785°C	Water quenched	500°C
A815O-T400	815°C	Oil quenched	400°C
A815O-T450	815°C	Oil quenched	450°C
A815O-T500	815°C	Oil quenched	500°C
A815W-T400	815°C	Water quenched	400°C
A815W-T450	815°C	Water quenched	450°C
A815W-T500	815°C	Water quenched	500°C

3.3 X-Ray Diffraction Analysis

For phase detection of the heat treated samples an X-ray diffraction (XRD) method was used with monochromatic Cu-Kα radiation (wavelength $\lambda = 1.54A^0$) at 40 kV and 100mA. Step size of 2Θ per minute and 2Θ range of (30-90) ° was applied. The recorded files were analysed to obtain the precise diffraction peak positions and integrated intensities planes.

Figure 3.3 X-Ray Diffraction

3.4 Optical Microscopy

Optical microscope was used to study the microstructures of as-cast and heat treated specimens.

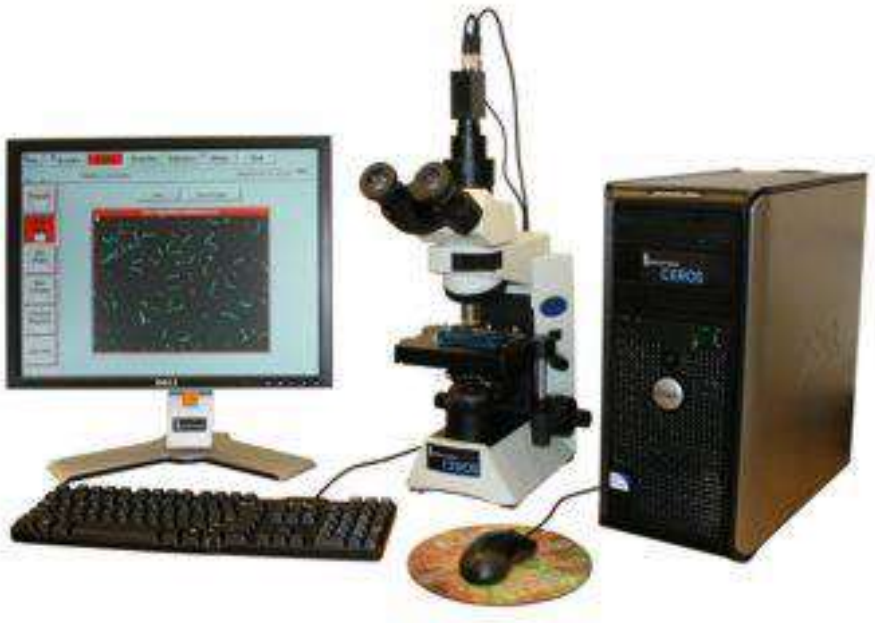

Figure 3.4 Metal power image analyser with optical microscope

3.4.1 Measurement of Ferrite and Martensite Volume Fraction

The martensite and ferrite volume fraction were determined using the analysis software-Metal power image analyser. The ferrite volume fraction (FVF) and martensite volume fraction (MVF) of DI with DMS were measured using point count method (ASTM E562-08).

3.5 Hardness Measurement

Hardness values of DI with DMS and quenched and tempered DMS samples were measured using Vickers hardness testing machine maintaining indentation load of 30 kg and dwell time of 10 s. Minimum 10 readings were taken for each specimen to obtain the average value.

Fig. 3.5(a) Vickers Hardness Tester

Vickers hardness tester uses a diamond indenter in the form of right pyramid with a square base. The angle is supposed to be 136^{o} between the opposite faces. Generally the results are reported in kg/cm^{2} which is proportional to the load divided by the square of the diagonal of the indentation calculated from the test. The load on the Vickers hardness indenter can be taken usually to kilograms. The resulting indentation is measured by the mathematical formula and converted to a hardness value. The test samples were polished before measuring the hardness.

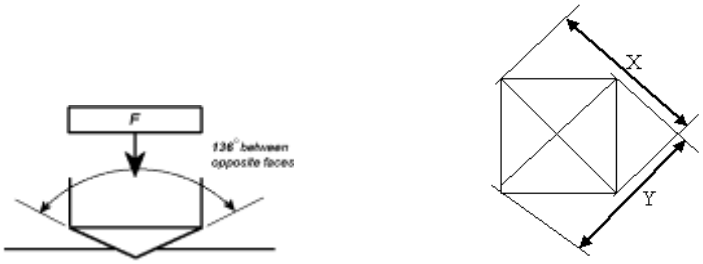

Fig. 3.5(b) Schematic figure of the Vickers pyramid diamond indentation

The two diagonals X and Y of the indentation left on the surface of the material after removal of the load are measured and their arithmetic mean L is calculated. Vickers hardness number is calculated using the following equation:

$$H_V = \frac{0.1889F}{L^2} \ldots (1)$$

$$L = \frac{X+Y}{2} \ldots . (2)$$

Where F is the applied load (N), L is the diagonal of square impression (mm), X is the horizontal length (mm) and Y is the vertical length (mm).

Microhardness of martensite was measured using Lecco Vickers Microhardness (LV 700) with a diamond indenter in the present investigation.

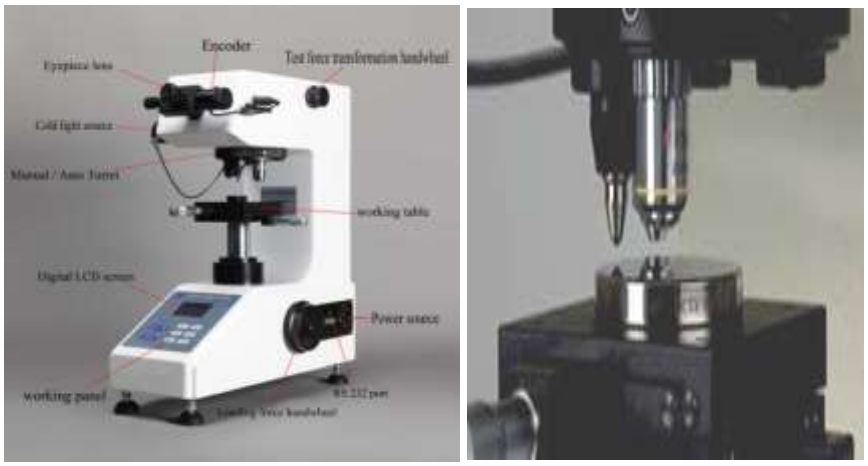

Figure 3.5 (c) Vickers Microhardness Tester

3.6 Tensile Testing

After machining to final dimensions the tensile test were carried out as per ASTM E-8. The test was performed on a computer integrated UTM (Instron 1195) with 100KN loading capacity at a cross head speed of 1mm min^{-1}. All of the samples were tested at room temperature and ambient atmosphere. The following procedure was adopted in ensuring that the data recorded from tensile test specimens was taken in an organised and consistent manner.

- Before loading the specimens in the Instron machine, the gauge length and width of respective specimens were fed into computer. The applied load and cross head speed for every test were maintained constant i.e., 50KN and 1mm/min respectively.
- The specimens were loaded into the Instron machine, and a tensile test was performed. After fracture of the specimens, the tensile strength, yield strength, and % elongation were recorded electronically and reported. Figure 3.6 gives a visual representation of the specimen nomenclature and the set-up used for testing.

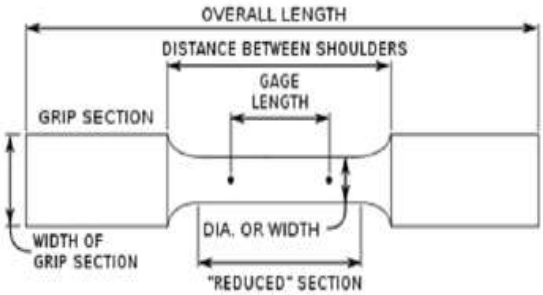

GRIP SECTION	1.25 Inch
WIDTH OF GRIP SECTION	3/8 Inch
GAUGE LENGTH	1±0.003 Inch
WIDTH	0.25±0.005 Inch
REDUCED SECTION	1.25 Inch
OVERALL LENGTH	4 Inch
THICKNESS	0.005≤T≤0.25 Inch

Figure: 3.6(a) Flat sub size specimen nomenclature, ASTM E-8.

Figure: 3.6 (b) Computer Integrated Instron 1195

3.7 Fractograhpy

The tensile fracture surfaces of all the tested samples were observed using Field Emission Scanning Electron Microscopy (FESEM).

Fig. 3.7 Field Emission Scanning Electron Microscopy

FEI *Nova Nano FEG-SEM 450* FESEM produces clearer, less electrostatically distorted images with spatial resolution down to 1.5 nm which is 3 to 6 times better than conventional SEM. Field Emission Scanning Electron Microscopy (FESEM) uses field-emission cathode in the electron gun of a scanning electron microscope. A field-emission cathode in the electron gun provides narrower probing beams at low as well as high electron energy, resulting in both improved spatial resolution and minimized sample charging and damage. High quality images are obtained with negligible electrical charging of samples using an accelerating voltages range from 0.5 to 30 kV. Also in FESEM the need for placing conducting coatings on insulating materials is virtually eliminated.

3.8 Wear test

Dry sliding wear test of the DMS ductile iron were carried out with a Ducom TR-208-M1 Ball-on-Plate type wear tester using a diamond intender. Unlubricated wear tests with a sliding distance of 7.54 m at a linear speed of 0.063 m/s were performed at room temperature with normal loads of 20N, 40N and 60N. A constant 4mm track diameter was used throughout the wear test. The weight loss for corresponding specimens were measured with the help of electronic balance of 0.1mg accuracy, prior to the weight measurement specimens were cleaned ultrasonically with acetone before and after the wear took place.

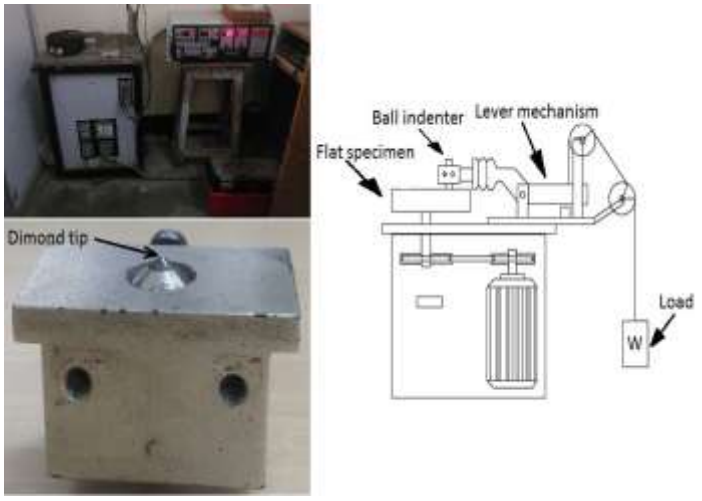

Figure 3.8 Ducom TR-208-M1 Ball-on-Plate Wear Tester

3.8.1 Worn surface analysis

The wear track and wear debris were observed under scanning electron microscopy.

Figure 3.9 Scanning Electron Microscopy

A JEOL -JSM-6480LV has been used in the present investigation. For Energy Dispersive X-Ray Spectroscopy (EDX) analysis, an INCAPentaFET-x3 x-ray microanalysis system with a high-angle ultra-thin window detector and a 30 mm^2 Si (Li) crystal was used.

…….

Chapter 4

Results and Discussion

Results and Discussion

4.1 X-Ray Diffraction Analysis

X-Ray Diffraction (XRD) was performed using monochromatic Cu-Kα radiation (wavelength λ = 1.54A^0) at 40 kV and 100mA. Step size of 2Θ per minute and 2Θ range of (30-90) ° was applied. Planes were used to determine the by matching d-spacing, 2Θ and the intensities of the peaks with help of database of expert high score software. From the figure 4.1 the major peaks are at angles 44.33°, 64.63° and 82.03° were obtained for the DI with DMS samples with minor difference in the 2Θ. This 2Θ-range contains the (110), (200) and (211) BCC planes suggesting ferrite and martensite phase. The results were used to figure out if some retained austenite existed in the DI with DMS samples. No retained austenite was detected in DI with DMS samples, since austenite had a FCC structure.

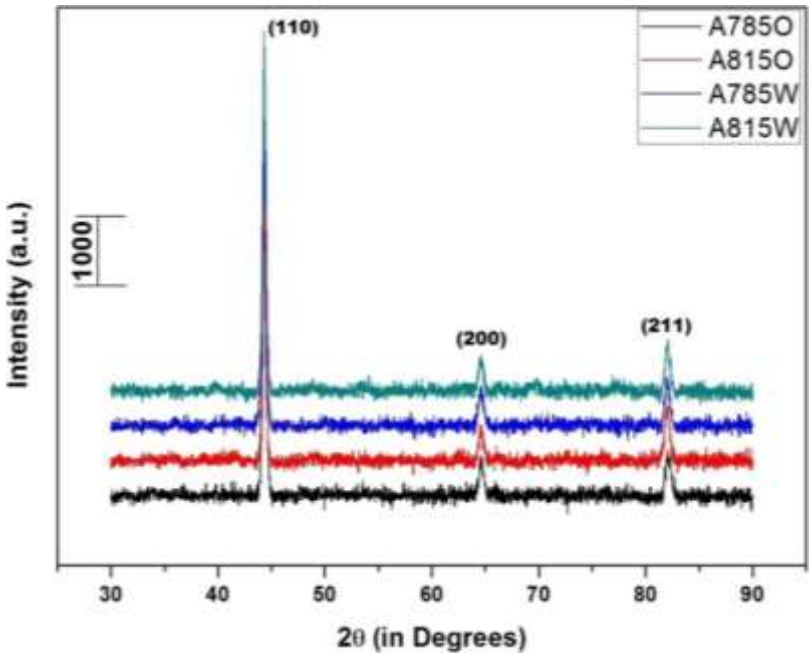

Figure 4.1 XRD plot for ductile iron with dual matrix structure samples.

4.2 Microstructure

Microstructure of the as-cast structure, DI with DMS (under different ICAT and quenching medium) and quenched and tempered DMS DI has been discussed in this section.

4.2.1 As-Cast Matrix Structure

The chemical composition and microstructure of ductile iron used in this study is given in Table 3.1 and Figure 4.2 respectively. The initial as-cast microstructure consisted of graphite nodules were embedded in ferrite matrix.

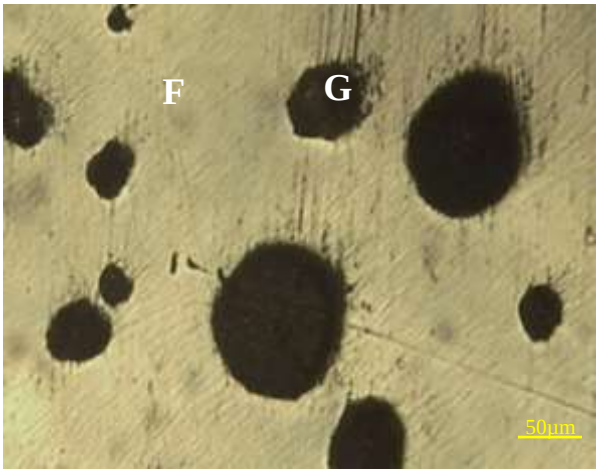

Figure 4.2 Microstructure of as-cast sample. F- Ferrite; G- Graphite.

4.2.2 Dual Matrix Structured Ductile Iron

The as-cast sample was intercritically austenitized at 785°C and 815°C quenched in oil and water. At ICAT of 785°C or 815°C the specimen remains in the austenite + ferrite region. On heating the as-cast matrix structure to the ICAT, austenite nucleated at prior ferrite/ferrite grain boundaries which are located in the eutectic cell and then grew into the ferrite. The quenching of the samples from different ICAT produced DMS with different ferrite and martensite volume fraction (Figure 4.3). The features of optical micrographs of treated as-cast DI samples and the influence of different ICAT and quenching medium are discussed below.

4.2.2.1 Influence of Intercritical Austenitizing Temperature and Quenching media

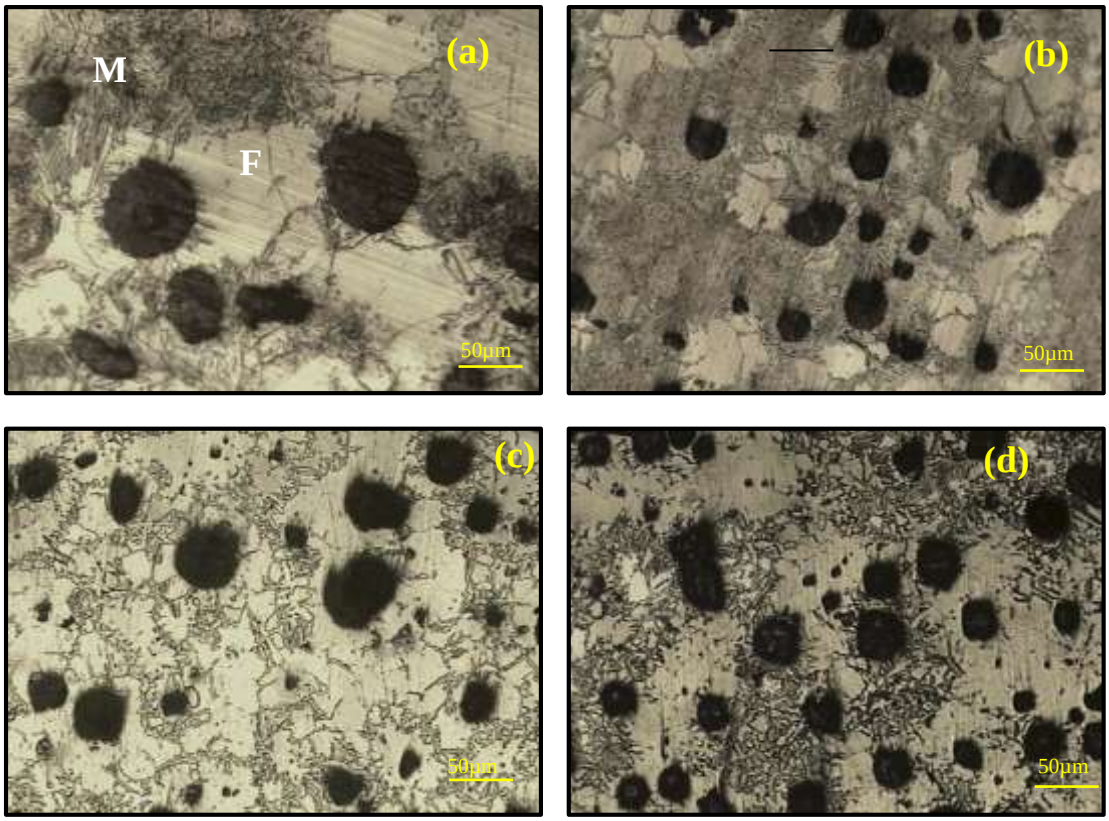

Figure 4.3 Microstructures of ductile iron with dual matrix structure for (a) A785W, (b) A815W, (c) A785O and (d) A815O. F- Ferrite; M- Martensite.

Figure 4.3 shows the microstructures of the ductile iron with dual matrix structure. It was observed that at ICAT of 785°C, the microstructure of A785W (Figure 4.3a) shows a quasi-continuous network of martensite structure along the ferrite grain boundaries and at a higher ICAT of 815°C, the microstructure of A815W (Figure 4.3b) shows a uniform network of martensite along the eutectic cells boundary. Since manganese (which is austenite stabilizer) segregates to the eutectic cell and only the minimum volume diffusion of carbon is needed for the nucleation of austenite, it is reasonable to assume that eutectic cells favours austenite nucleation. Considering the influence of quenching medium it is observed that the water quenched DI with DMS samples (Figure 4.3a and 4.3b) shows increased martensite connectivity whereas the oil quenched DI with DMS samples (Figure 4.3c and 4.3d) produce fine, well-dispersed, random, fibrous martensite particles in ferrite.

These results can be explained from the Figure 4.4 where ferrite volume fraction (FVF) decreases and martensite volume fraction (MVF) increases with the increase in ICAT range. In addition to that, it was found that water quenched DI with DMS samples have higher MVF then the oil quenched DI with DMS samples. Since martensite transformation occurs at high cooling rates, this result may be attributed to the high quenching severity in water quenching media as compared to the oil quenching media having relative density of 0.86. [11, 32, 36, 64]

Figure 4.4 shows the dependence of FVF and MVF on intercritical austenitizing temperature. This complies with the lever rule in the ferrite-austenite dual phase region. When the ICAT increases, the austenite volume fraction and its carbon content increases and FVF decreases (Figure 4.4a) and MVF increases (Figure 4.4b) as evident from applying lever rule in the intercritical region of the iron-carbon-silicon phase diagram. This means that MVF and FVF can be controlled by using this heat treatment since parent austenite formed during intercritical austenitizing transforms into martensite upon quenching. [31, 65]

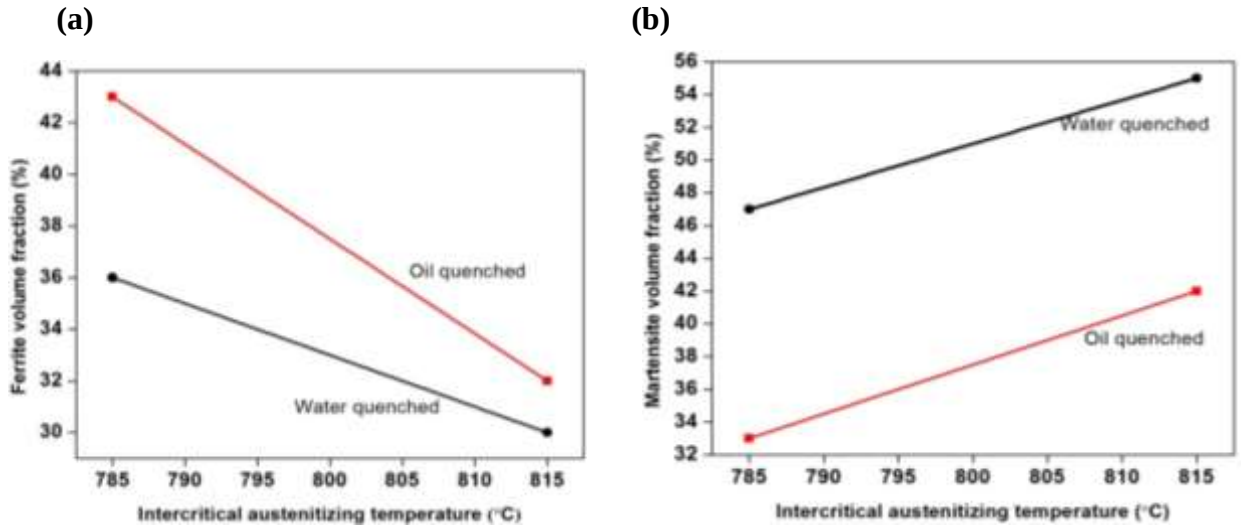

Figure 4.4 Dependence of (a) Ferrite Volume Fraction and (b) Martensite Volume Fraction on intercritical austenitizing temperature

4.2.2.2 Influence of Tempering Temperature

The DMS samples were tempered at different tempering temperatures. In the previous works that have been conducted in this area, all the authors concurred that tempering time of 1 hour is best for

these tempering temperatures, so in this study we concentrated on tempering time of 1 hour. The microstructures of quenched and tempered DI with DMS samples tempered at 400°C, 450°C and 500°C for 1 hour have been shown in Figure 4.5

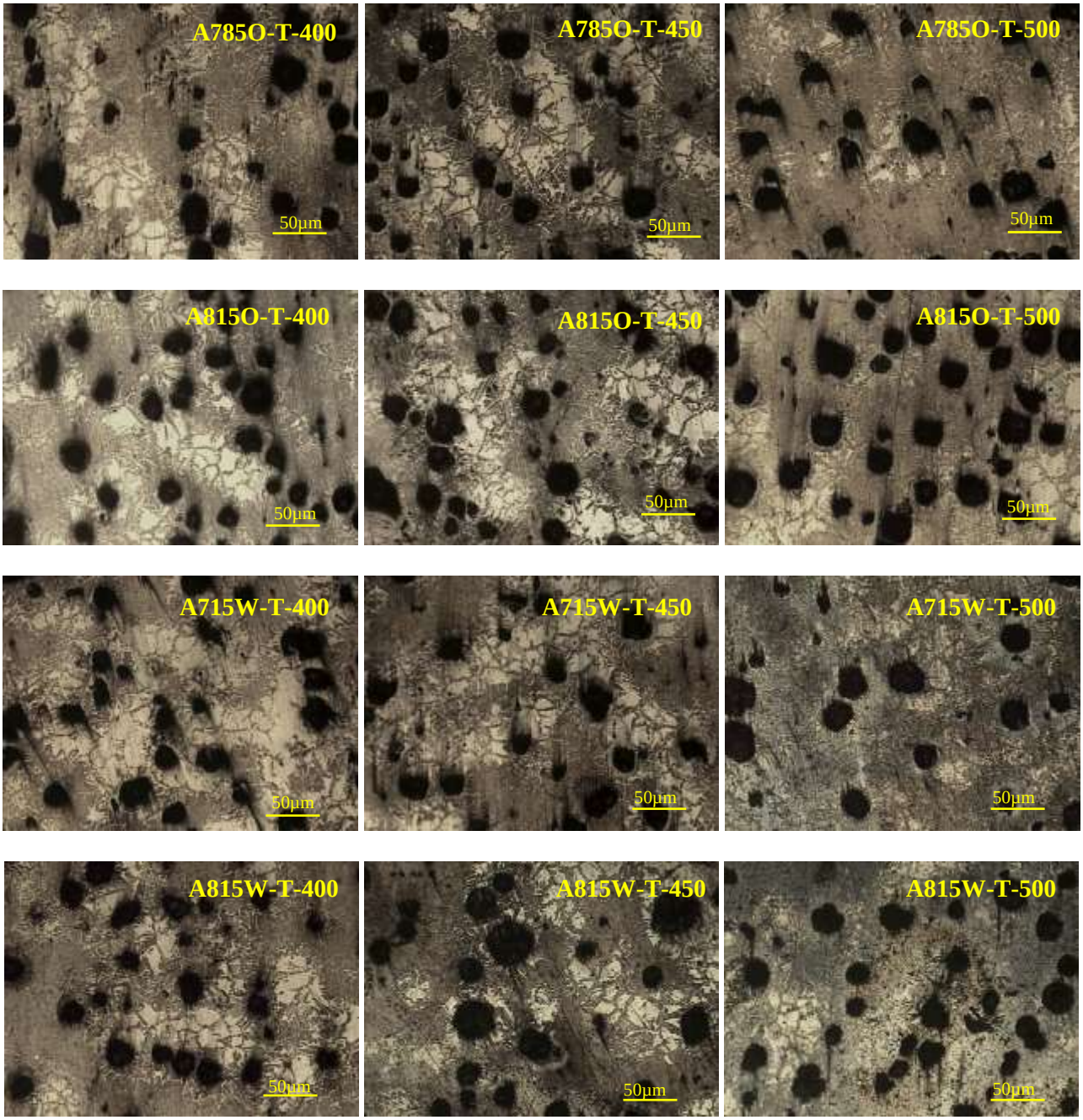

Figure: 4.5 Microstructures of quenched and tempered ductile iron with dual matrix structure samples at tempering temperatures of 400°C, 450°C and 500°C.

The microstrucutre of quenched and tempered DI with DMS specimens provides a microstructure of graphite nodules in a matrix of ferrite and tempered martensite particles. The specimens tempered at 400°C differs slightly from the untempered samples. Once the tempering temperature increases to

450°C, the microstructure shows dark tempered martensite phase embedded in ferrite matrix due to the precipitation of transition carbides. With a further increase in the tempering temperature to 500°C, the surface is characterised by the recovery of the defect structure in the martensite phase and precipitation of carbides. Furthermore, it causes carbon segregation into dislocations and precipitation of carbides in the ferrite phase. Formation of martensite generates residual stresses and a high dislocation densitiy in the ferrite especially near the martensite ferrite interface. Carbon segregation into these dislocations and the relief of the residual stresses by the volume contraction of the martensite phase during tempering are important parts of tempering process. [56, 66]

4.3 Mechanical Properties

The dependence of mechanical properties on intercritical austenitizing temperature, quenching media and tempering conditions depended upon the nature and amount of phases present. One of the major controlling parameter for mechanical properties of ductile iron with dual matrix structure is carbon content of the martensite. The micro hardness variation in martensite with ICAT in quenched samples from ICAT range is given in Figure 4.6. The micro hardness of martensite increases with the increase in ICAT. The dependence of the micro hardness of martensite on ICAT is a good indication of the martensite carbon content due to diffusion less nature of the austenite-martensite transformation [31, 59].

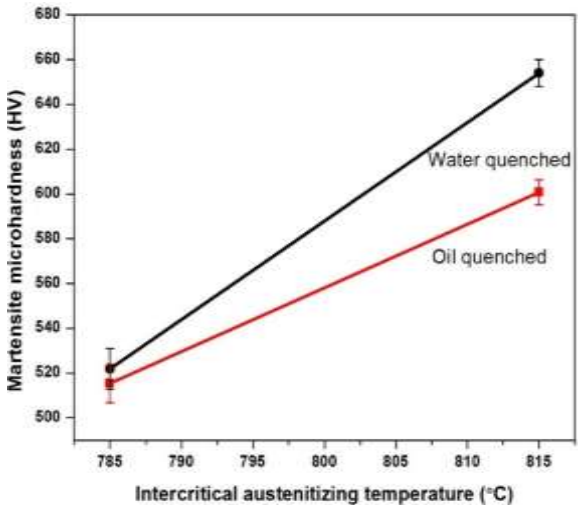

Figure: 4.6 Dependence of martensite microhardness on intercritical austenitizing temperature

4.3.1 Influence of Intercritical Austenitizing Temperature and Quenching media

The variations of ultimate tensile strength, yield strength, elongation and hardness with different ICAT and quenching medium are shown in Figure 4.7 (a-d).

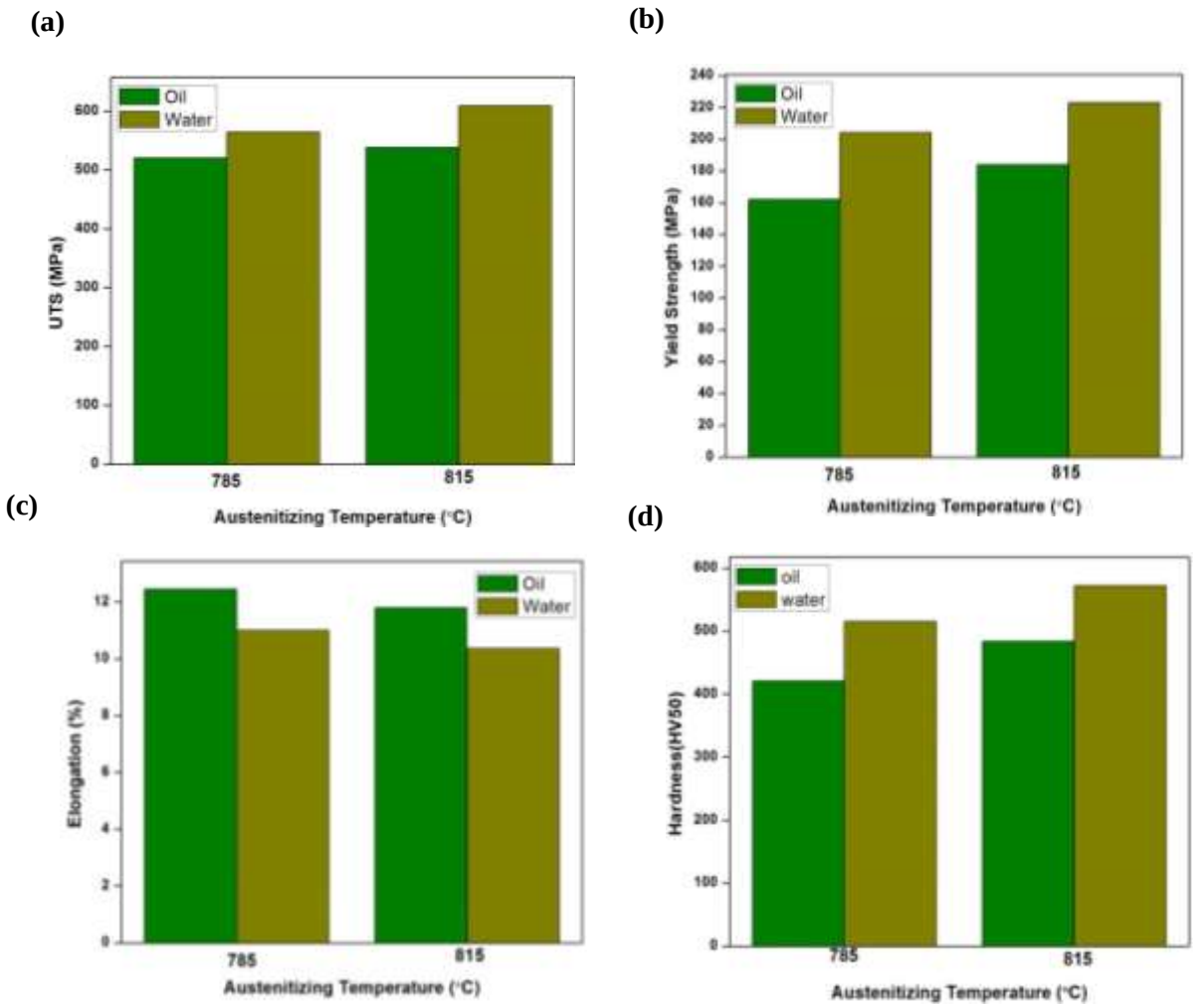

Figure 4.7 Effect of intercritical austenitizing temperature and quenching media on (a) Ultimate Tensile Strength (b) Yield Strength (c) Elongation % and (d) Hardness of ductile iron with dual matrix structure

In Figure 4.7 (a) and (b), it is apparent that both ultimate tensile strength (UTS) and yield strength (YS) increases with the increase in ICAT range. Irrespective of ICAT, the water quenched samples provides greater UTS and YS than the oil quenched samples. This result is attributable to the increase of MVF and decrease of FVF with the increasing ICAT range and the degree of quenching severity. The sample A815W shows the highest UTS and YS values owing to its highest value of MVF among

the other samples. As far as ductility is concerned, Figure 4.7 (c) shows the elongation decreases with the increase of ICAT range and decrease of FVF. This result demonstrates that the introduction of ferrite is a further means of controlling the mechanical properties of DI with DMS. The peak elongation occurs for A785O specimens in which the martensite particles are arbitrarily scattered in the ferrite matrix. The level of continuity of the martensite structure network along the intercellular boundary could be an essential parameter deciding the degree of ferrite deformation along the graphite nodules. In the specimen with higher MVF, the ferrite around the graphite nodules is totally encompassed by the martensite structure. In such a microstructure, high strength martensite structure may limit deformation of a larger fraction of the total volume of the low strength ferrite under tensile loading. Accordingly, the ductility increments with the decreasing progression of martensite structure along eutectic cell boundaries. Figure 4.7(d) shows that the hardness increases with the increasing of ICAT range and increasing carbon content in martensite. The specimen A815W, having the highest martensite carbon content provides the best hardness value among all other DMS samples [67, 68, 69].

4.3.2 Influence of Tempering Temperature

The variations of ultimate tensile strength, yield strength, elongation and hardness of quenched and tempered DI with DMS at various tempering temperature of 400°C, 450°C, and 500°C are shown in Figure 4.8 (a-d)

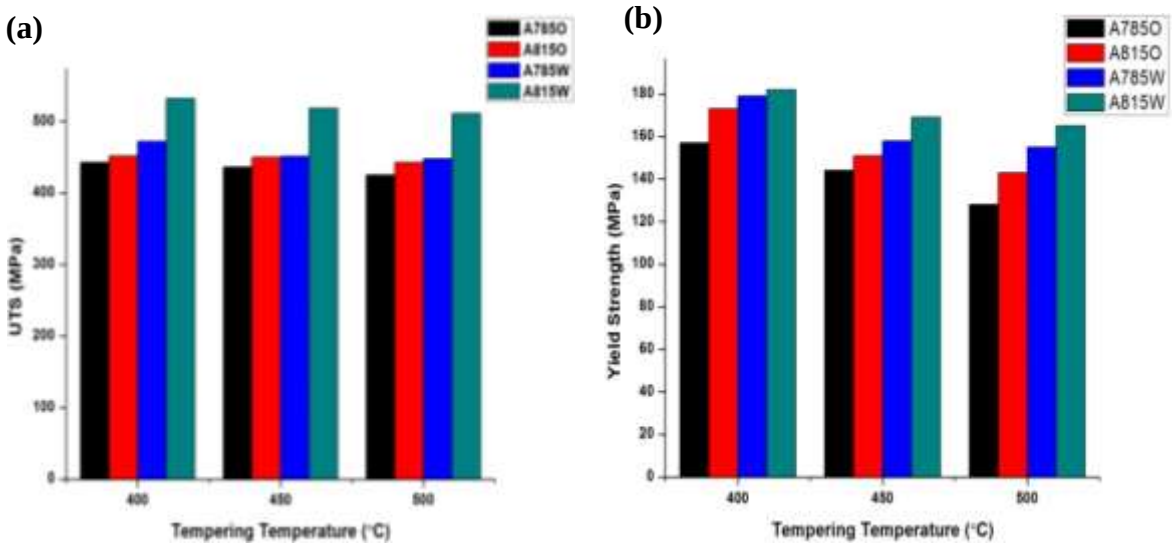

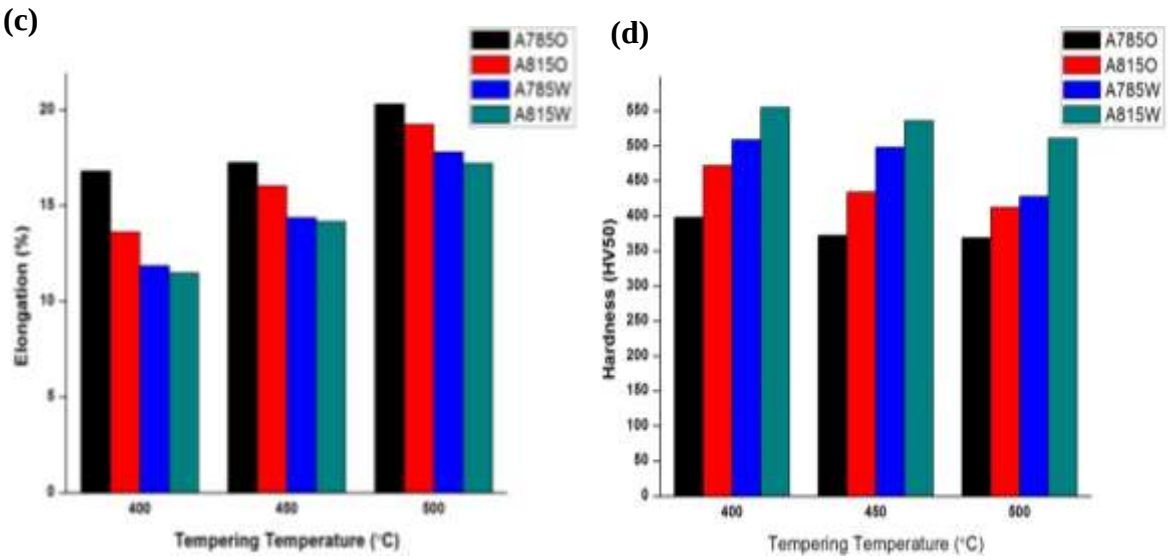

Figure: 4.8 Effect of tempering temperatures on (a) UTS (b) Yield strength (c) Elongation and (d) Hardness of quenched and tempered dual matrix structure ductile iron.

Figure 4.8 (a-b) demonstrates that by the increasing tempering temperatures, the UTS and YS initially decrease, then within the range of 450°C-500°C, remain almost constant due to the strain hardening which results due to the precipitation of fine dispersed complex carbides. Further increase in the tempering temperature results in the reduction of the strength difference between tempered martensite and ferrite. Figure 4.8 (c-d) shows that elongation increases and hardness decreases with the increase in tempering temperatures. This outcome can be credited to the excess carbon in the solution which diffuses to pin the free dislocations in the ferrite and form fine iron carbides. By increasing the tempering temperature from 400°C, most of the residual stresses are eased, the martensite phase is softened and, thus the elongation is increased. The specimen A815O-T450 shows the best combination of tensile strength (up to 518 MPa) and elongation (up to 15.6%) among all the treated quenched and tempered DI with DMS samples. [8, 36, 56, 70-74]

4.4 Fractography

The fracture mechanism of the specimens was analyzed based on examination of the fracture surfaces under FESEM. Figure 4.9 shows the FESEM micrographs of DMS tensile samples fractured at room temperature.

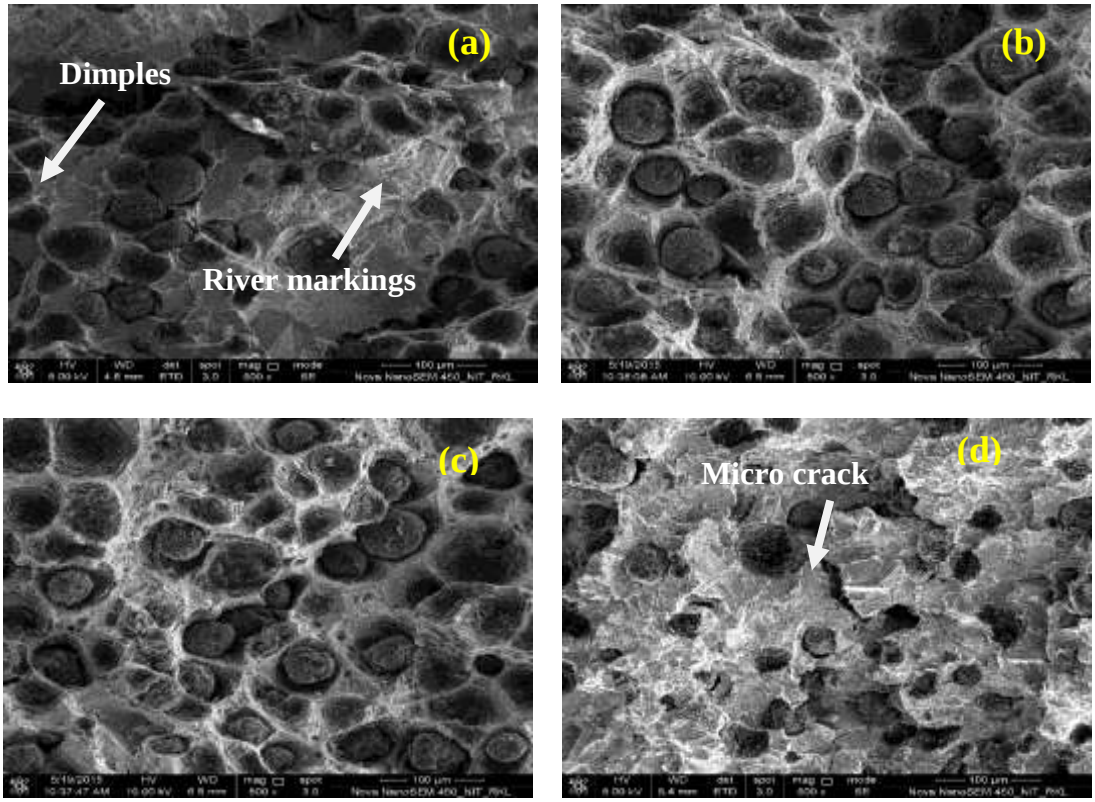

Figure: 4.9 Fractography of tensile fractured surface of ductile iron with dual matrix structure sample (a) A785O (b) A815O (c) A785W and (d) A815W

The FESEM observation of the fracture surface (Figure 4.9) shows that there is a combined mechanism of dimple rupture and river markings together. This sort of fracture is called quasi-cleavage fracture. In the fracture surface micrographs, the cavity size in comparison with the graphite nodules is a decent sign of the deformability of DI with different MVF. Development of cavity may be ascribed to decohesion at the graphite and the surrounding matrix. The dimple pattern around the graphite nodules show the deformation of the surrounding ferrite amid the final period of straining up to fracture. The fracture surface of oil quenched samples (Figure 4.9a and 4.9b) shows mainly dimple depression reflecting dominant ductile nature since the ferrite fails in a more ductile fashion and its commitment to the fracture resistance increments with the increasing FVF. The fracture surface of the specimen A785O (Figure 4.9a) having highest FVF reveals more uniform equiaxed dimple depressions along the graphite nodules compared to other DMS specimens confirming the highest elongation percent. For the specimen A815O (Figure 4.9b) the clearances

between the graphite nodules and their corresponding cavities changes from larger to tighter with increasing MVF. The little leeway demonstrates slight occurrence of plastic deformation around the graphite nodules. As the network of martensite structure along the intercellular boundaries in the matrix increases with the increasing MVF, this structure confines plastic flow of soft ferrite to higher extent. Therefore ductility decreases compared to A785O specimens. Furthermore, the water quenched samples (Figure 4.9c and 4.9d) having low amount of FVF compared to oil quenched samples shows mainly the river pattern, expressing dominant brittle fracture. In addition, fracture surface of the specimen A815W (Figure 4.9d) having the highest MVF value shows a micro-crack formed at the graphite-matrix interface reflecting high strength of the sample. This result is in good agreement with the mechanical properties of DI with DMS. [67, 75, 76]

Figure 4.10 shows the FESEM micrographs of quenched and tempered tensile DI with DMS samples fractured at room temperature.

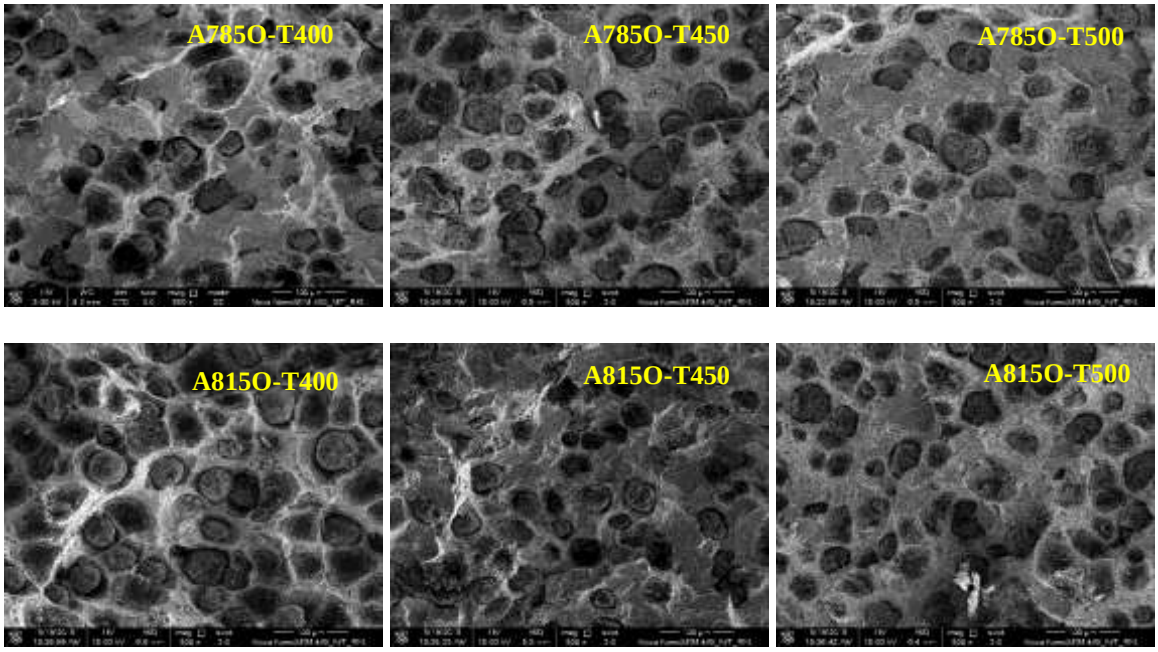

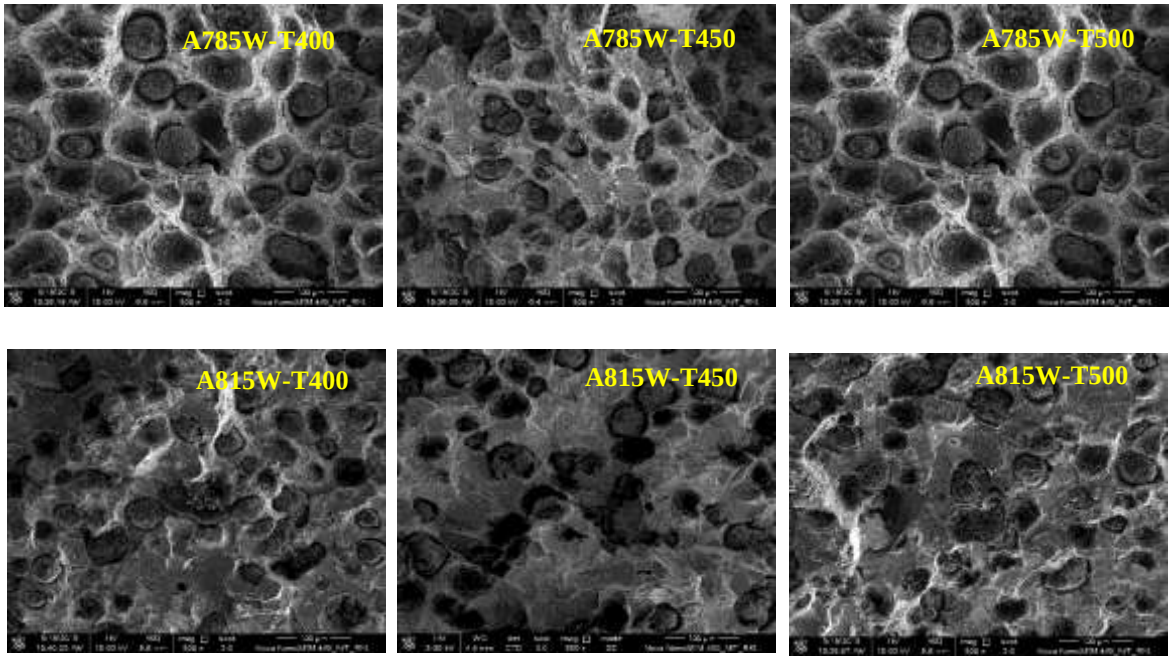

Figure 4.10 Fractography of tensile fractured surface of Quenched and Tempered Ductile Iron with Dual Matrix Structure samples.

In Figure 4.10, the tensile fracture surface of DMS specimens tempered at 400°C, 450°C and 500°C is shown. All samples exhibited a cleavage type fracture characterised by river markings and dimples but the nature of the fracture changes significantly with tempering temperatures. At tempering temperature of 400°C, the fracture surface is mainly brittle as revealed by the presence of river markings and cleavage facets due to the presence of tempered martensite. Only some areas consist of dimples due to the presence of ferrite matrix. This observation is consistent with the mechanical properties of tempered samples at 400°C tempering temperatures which show highest strength and lowest elongation among the other tempered samples. With the increase in tempering temperature to 450°C the fracture surface shows dominant ductile dimples along with few cleavage facets. As the tempering temperature increases, most of the residual stresses is relieved the martensite phase is softened and hence UTS and YS decreases. At a higher tempering temperature of 500°C the martensite phase gets more soften and hence the fracture surface reveals mostly ductile nature with rarely encountered small areas showing cleavage justifying its highest degree of ductility among all other tempered samples. [70]

4.5 Wear Properties

The effects of varying loads in DI with DMS and quenched and tempered DI specimens were investigated for various intercritical austenitizing temperatures and quenching media and tempering temperatures. The weight loss of the samples was determined and is presented graphically in Figure 4.11 and 4.12 as a function of applied loads.

4.5.1 Influence of Intercritical Austenitizing Temperature and Quenching media

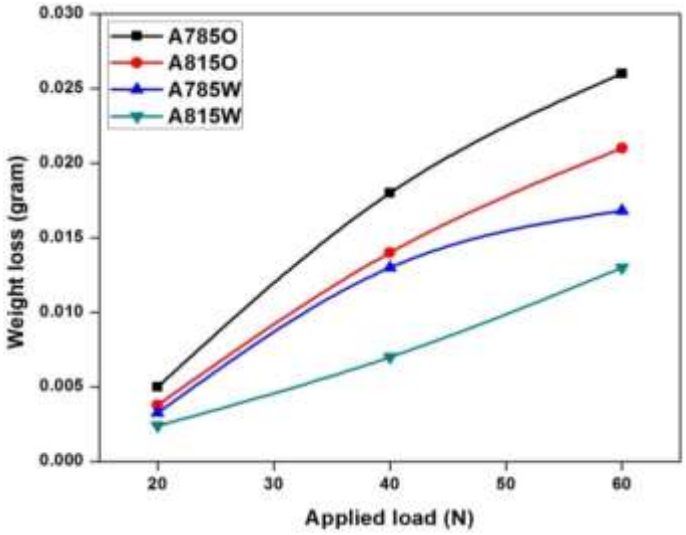

Figure 4.11 Graphical representation of weight loss as a function of applied load for ductile iron with dual matrix structure samples.

Figure 4.11 shows the variation of weight loss as a function of applied load for the specimens intercritically austenitized at temperatures 785°C and 815°C quenched in various quenching mediums oil and water. It could be seen that the weight loss of samples intercritically austenitized at 815°C is lower than that of the samples intercritically austenitized at 785°C with same quenching medium irrespective of all loads due to the changes in MVF and hardness. It means that the ICAT influences the wear behaviour of DI samples. This might be attributable to the increasing MVF and increasing hardness of the samples with the increase in ICAT. Considering the quenching medium it is observed that the weight loss of the water quenched samples was less than the oil quenched samples. This might be due to the increased connectivity of martensite network structure compared to oil quenched samples. Furthermore, the weight loss of all the samples tested increased as the applied

load was increased since an increment in the load might increase the contact stress leading to further surface damage.

However, the lowest weight loss was obtained for the sample A815W probably due to the presence of a uniform network of martensite throughout the specimen having the highest MVF (55%). The high strength martensite phase might limit the wear of low strength ferrite matrix resulting in minimum weight loss. The largest weight loss was obtained with increasing load for the sample A785O probably due to the presence of lower MVF (33%) and higher FVF (43%). It may be due to the increase of ductility with the decreasing continuity of martensitic structure along the eutectic cells. [61, 77]

4.5.2 Influence of Tempering Temperature

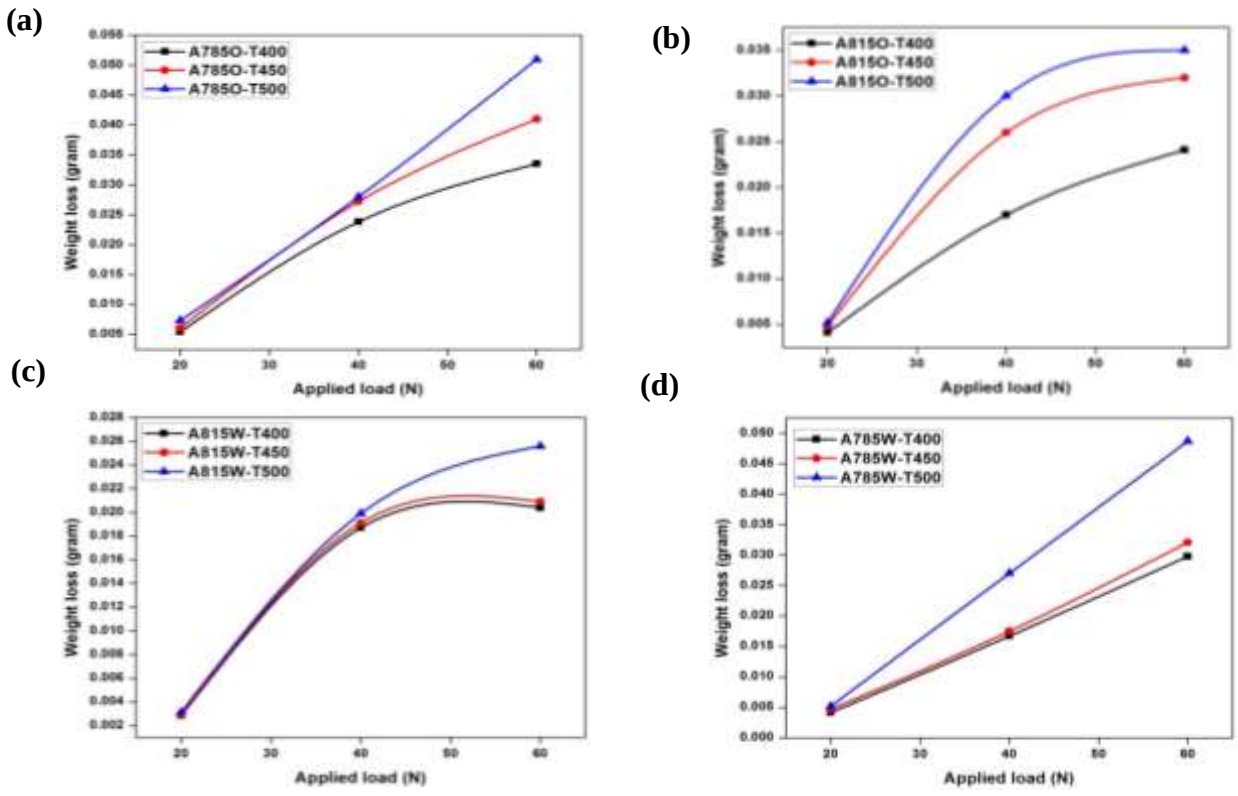

Figure 4.12 Graphical representation of weight loss as a function of applied load for quenched and tempered ductile iron with dual matrix structure samples (a) A785O, (b) A815O, (c) A785W, and (d) A815W quenched and tempered at different tempering temperatures of 400°C, 450°C and 500°C.

Figure 4.12 shows the variation of weight loss as a function of applied load for quenched and tempered DMS samples at 400°C, 450°C and 500°C. It could be seen that among the tempered DI with DMS samples weight loss at tempering temperature of 500°C is maximum, and the DI with DMS samples tempered at 400°C exhibits least weight loss. At tempering temperature of 450°C tempered DI with DMS sample shows intermediate wear response. Since with the increasing tempering temperature from 400°C, most of the residual stresses are relieved and the martensite phase gets soften and, hence the weight loss increases. In figure 4.12(a), at applied load of 20N, the weight loss difference among all tempered DI with DMS samples of A785O is very less due to the minimum contact stress at low load. The difference in weight loss between A785O-T400 and A785-T450 was pronounced beyond 40N due to the larger difference in hardness values from tempering temperatures 400°C to 450°C, whereas, the difference in weight loss between A785O-T450 and A785O-T500 is very small due to the smaller difference in the hardness values. Similar trend is observed for the DI with DMS sample A815O quenched and tempered at tempering temperatures of 400°C, 450°C and 500°C in Figure 4.12(b) explained on the basis of hardness difference at different tempering temperatures. In Figure 4.12(c), the difference in weight loss for the tempered DI with DMS samples A785W-T400 and A785W-T450 is very less as because the difference in hardness value is very small whereas, the difference in weight loss between the tempered DI with DMS samples A785W-T450 and A785W-T500 is significant because of the large increase in hardness value from tempering temperatures 450°C to 500°C as seen in Figure 4.8(c). Similar observation was made for tempered DI with DMS samples A815W quenched and tempered at 400°C, 450°C and 500°C in Figure 4.12(d). [59]

4.6 Worn Surface Investigation

The SEM images of worn surface of the different DI with DMS samples and quenched and tempered DI with DMS samples are discussed in this section.

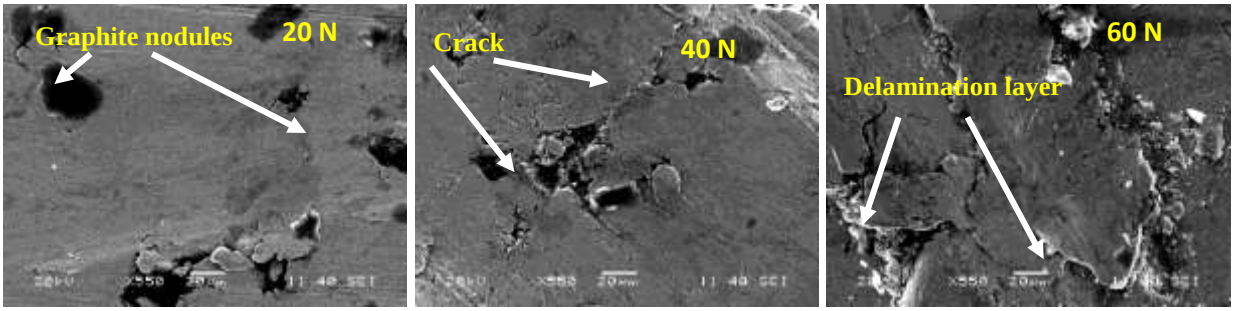

(a) A785O

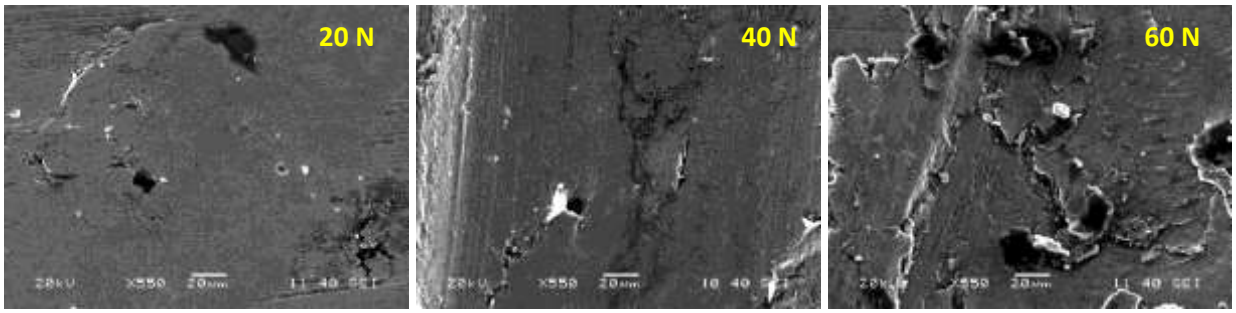

(b) A815O

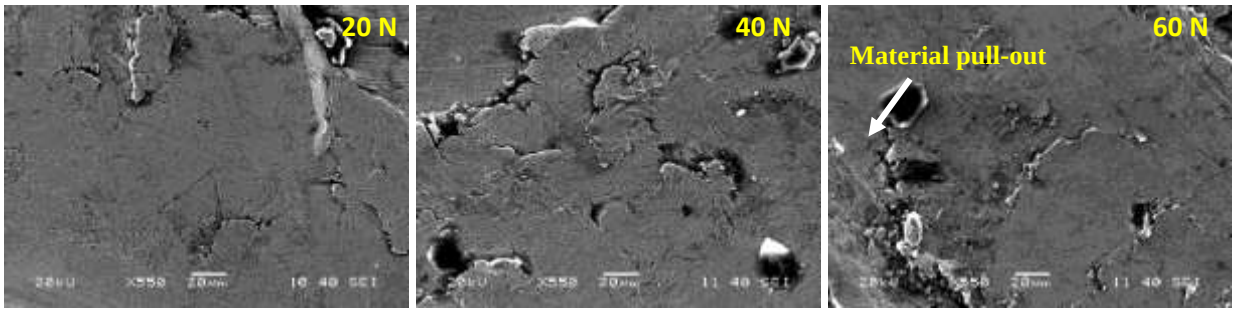

(c) A785W

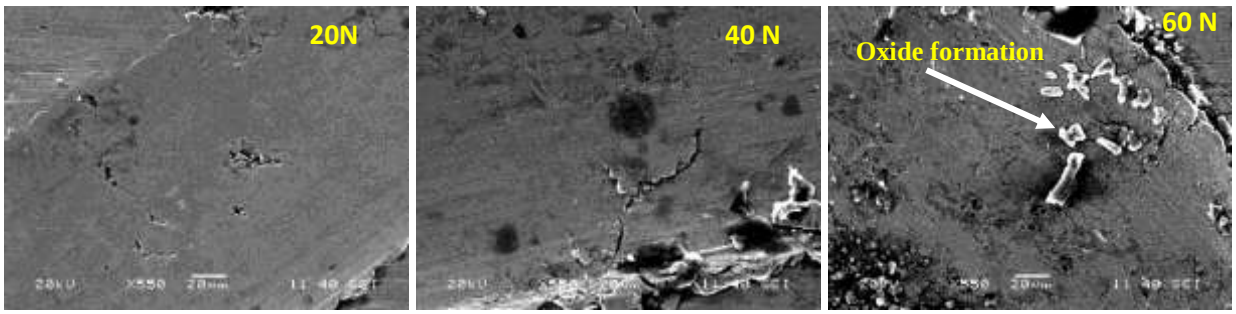

(d) A815W

Figure 4.13 SEM images of worn surface at various loads of 20N, 40N, 60N for ductile iron with dual matrix structure sample (a) A785O (b) A815O (c) A785W and (d) A815W

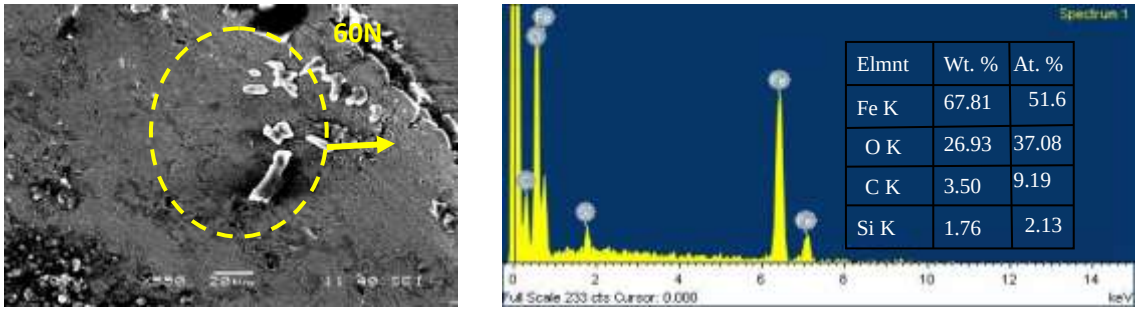

Figure 4.14 EDAX analysis of the worn surface at 60N load for ductile iron with dual matrix structure sample A815W.

Figure 4.13 shows the worn surface morphologies under various loads of the DI with DMS samples. It can be found that the wear is mainly caused by delamination of subsurface, presence of voids and micro cracks suggesting adhesive nature of the worn surface. Under lower applied load of 20N, the worn surface of all the tested samples presents almost smooth surface with small delamination crater. When the load increases to 40N, the worn surface shows rough surfaces with significant delamination damage. On increasing the load to 60N, the worn surface shows intensively severe delamination damage and more material pull-out was observed. Meanwhile, at 60N some oxidized particles are evident due to generation of heat at higher applied load as seen in Figure 4.14. Obviously, the highest wear scar was observed for the sample A785O (Figure 4.13a) at each loads compared to other DI with DMS samples. The surface of the graphite nodule was almost covered by the deforming and smearing of the material which is the indication of more ductile nature. The worn surface for the sample A815W (Figure 4.13d) shows a better maintained surface with relatively slight delamination due to higher hardness and increased MVF which resist the initiation and propagation of cracks. The delamination mechanism involves nucleation of cracks at the interface of ferrite and martensite. Increasing the volume fraction of martensite decreases the interface of ferrite and martensite and therefore, the number of suitable places for nucleation and propagation of crack decreases. Moreover, this sample shows some amount of oxide formation (Figure 4.13d) at 60N load confirmed by the EDX analysis (Figure 4.14)

indicating more brittle nature of the material compared to other tested DMS which is consistent with the fractography result. [77-79]

To study the wear mechanism influenced by different tempering temperatures, the SEM images of worn surface of quenched and tempered DI with DMS (A785O) sample is considered for the investigation.

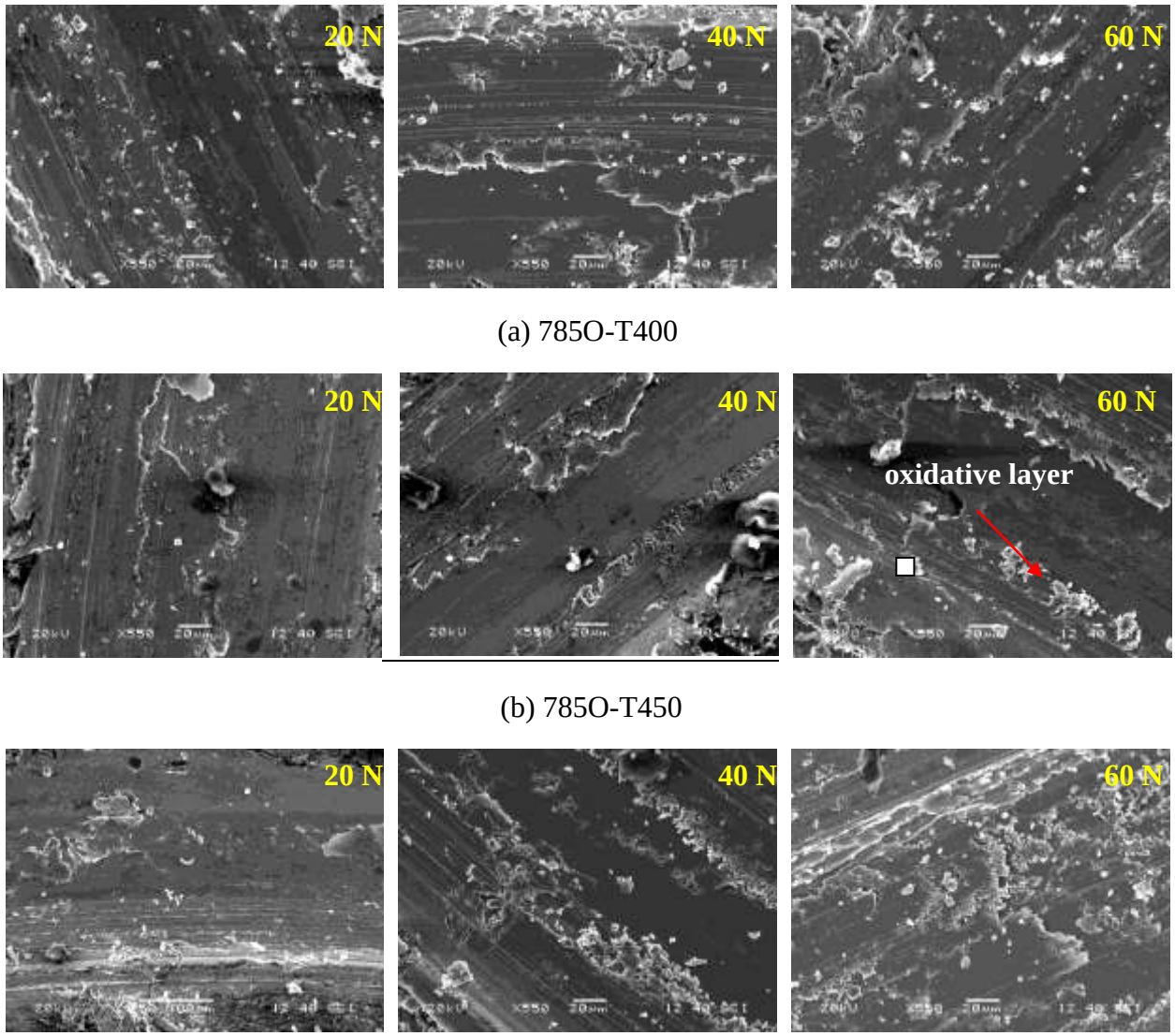

Figure 4.15 SEM images of worn surface at various loads of 20N, 40N, 60N for quenched and tempered ductile iron with dual matrix structure sample (a) A785O-T400 (b) A785O-T450 and (c) A785O-T500

Figure 4.15 shows the SEM images of worn surface for quenched and tempered DMS A785O sample tempered at 400°C, 450°C and 500°C under various loads 20N, 40N, and 60N. It can be observed the wear mechanism involves a mixed oxidative layer and delaminated region on the worn surface. The degree of of oxide layer increases with increase in applied load. In Figure 4.15(a) the worn surface at 400°C shows relatively smooth surface with minimum wear scar compared to other tempering temperature due to the high strength and hardness value of the sample A785O at 400°C. In Figure 4.15 (b) the worn surface at 450°C was more rough and propagation of cracks was evident which produces a significant delaminated layer along with discontinous oxide layer since with the increase in tempering temperature most of the residual stress gets relieved and martensite phase gets softens. In Figure 4.15(c) the worn surface gets more rougher with intense delaminated layers and a cover of oxide layer was evident. This may be due to the decreased strength and hardness value and increased ductility of the sample A785O-T500 with the increasing tempering temperature from 450°C to 500°C [59, 80-82].

……..

Chapter 5
Conclusions

Conclusions

This thesis reports the results of a systematic study of influence of intercritical autenitizing temperatures and quenching medium and tempering temperatures on mechanical properties and wear behaviour of dual matrix structured ductile iron. The conclusions drawn from the present investigation are as follows:

1. Intercritical austenitizing heat treatment adopted in this study produced a dual matrix microstructure in ductile iron comprising of ferrite and martensite. The ductile iron so treated is called dual matrix structured ductile iron. Ferrite and martensite volume fractions can be controlled to influence the strength and ductility of ductile iron with dual matrix structure
2. For the DMS DI samples martensite volume fraction increases and ferrite volume fraction decreases with the increase in intercritical austenitizing temperature and degree of quenching severity.
3. Ultimate tensile strength, yield strength increases and ductility decreases with the increase in martensite volume fraction and decrease in ferrite volume fraction. Micro hardness of martensite phase increases with the increase in intercritical austenitizing temperature.
4. With the increasing tempering temperatures, the ultimate tensile strength and yield strength initially decreases, then within the range of 450°C-500°C, remain roughly constant. The elongation increases and hardness decreases with the increase in tempering temperature from 400°C to 500°C.
5. The different fracture mechanism corresponds to the different level of martensite volume fraction and observed mechanical properties. Fractrographic examination shows that DMS DI samples fails in quasi-cleavage fashion. Fracture pattern for the

quenched and tempered DMS samples changes from brittle to moderate ductile fracture with increase in tempering temperature.

6. The weight loss of the DMS samples decreases with the increase in intercritically austenitized temperature and martensite volume fraction. Among the tempered DMS samples weight loss at tempering temperature of 500°C is maximum, and the DMS samples tempered at 400°C exhibits least weight loss.
7. The weight loss of all the tested samples increased as the applied load was increased since an increase in the load might increase the contact stress thus resulting in further surface damage.
8. The worn surface of DMS DI was mainly caused by delamination of subsurface, presence of voids and micro cracks suggesting adhesive wear mechanism. Whereas, the wear mechanism of tempered DMS samples involves a mixed oxidative layer and delaminated region on the worn surface.

……..

References

[1] Morrogh, H. "Production of nodular graphite structures in gray cast irons." *AFS Transactions* 56 (1948): 72.

[2] Verhoeven, John D. *"Steel metallurgy for the non-metallurgist*." ASM International, (2007).

[3] http://www.afsinc.org/files/Dec13%20Census.pdf

[4] Kobayashi, T. "Ductile Cast Iron." *In Strength and Toughness of Materials*, Springer Japan, (2004): 89-110.

[5] Hasan, Avdusinovic, Almaida Gigovic, Nermin Mujezinovic, and Cimos TMD Casting. "AUSTEMPERED DUCTILE IRON."

[6] Mullins, James D. "Ductile iron data for design engineers." *Rio Tinto Iron & Titanium Inc.* (1990).

[7] Voigt, R. C., L. M. Eldoky, and H. S. Chiou. "Fracture of ductile cast irons with dual matrix structures." *Transactions of the American Foundrymen's Society*.94 (1986): 645-656.

[8] Rashidi, Ali M., and M. Moshrefi-Torbati. "Effect of tempering conditions on the mechanical properties of ductile cast iron with dual matrix structure (DMS)."*Materials Letters* 45(3) (2000): 203-207.

[9] He, Z. R., G. X. Lin, and S. Ji. "Deformation and fracture of cast iron with an optimized microstructure." *Materials characterization* 38(4) (1997): 251-258.

[10] Hafiz, Mahmoud. "Tensile properties and fracture of ferritic SG-iron having different graphite-shell structure." *Zeitschrift für Metallkunde* 92(11) (2001): 1258-1261.

[11] Kobayashi, Toshiro, and Hironobu Yamamoto. "Development of high toughness in austempered type ductile cast iron and evaluation of its properties." *Metallurgical Transactions A* 19(2) (1988): 319-327.

[12] Kobayashi, Toshiro, and Shinya Yamada. "Effect of holding time in the (α+ γ) temperature range on toughness of specially austempered ductile iron."*Metallurgical and materials Transactions A* 27(7) (1996): 1961-1971.

[13] Nofal, Adel. "Advances in the metallurgy and applications of ADI." *Journal of Metallurgical Engineering (ME)* 2(1) (2013).

[14] Islam, M. A., A. S. M. A. Haseeb, and A. S. W. Kurny. "Study of as cast and heat treated spheroidal graphite cast iron under dry sliding conditions." *Wear* 244 (2000): 15-19.

[15] Ahmadabadi, M. Nili, H. M. Ghasemi, and M. Osia. "Effects of successive austempering on the tribological behavior of ductile cast iron." *Wear* 231(2) (1999): 293-300.

[16] Cueva, G., A. Sinatora, W. L. Guesser, and A. P. Tschiptschin. "Wear resistance of cast irons used in brake disc rotors." *Wear* 255(7) (2003): 1256-1260.

[17] Islam, M. A., A. S. M. A. Haseeb, and A. S. W. Kurny. "Study of wear of as-cast and heat-treated spheroidal graphite cast iron under dry sliding conditions." *Wear* 188(1) (1995): 61-65.

[18] Prado, J. M., A. Pujol, J. Cullell, and J. Tartera. "Dry sliding wear of austempered ductile iron." *Materials Science and Technology* 11(3) (1995): 294-298.

[19] Hatate, M., T. Shiota, N. Takahashi, and K. Shimizu. "Influences of graphite shapes on wear characteristics of austempered cast iron." *Wear* 251(1) (2001): 885-889.

[20] Avner, Sidney H. "Introduction to physical metallurgy." (1964).

[21] Callister, William D., and David G. Rethwisch. *Materials science and engineering: an introduction*." New York: Wiley, 7 (2007).

[22] Angus, Harold T. *Physical and Engineering Properties of Cast Iron: A Data Book for Engineers and Designers*. British Cast Iron Research Association, (1960).

[23] Elliott, Roy. *Cast iron technology*. Butterworth-Heinemann, (1988).

[24] Durand-Charre, Madeleine. *Microstructure of steels and cast irons*. Springer Science & Business Media, (2004).

[25] Kenawy, M. A., A. M. Abdel-Fattah, N. Okasha, and M. EL-Gazery. "Mechanical and Structural Properties of Ductile Cast Iron." *Egypt Journal of Solidification* 24(2) (2001).

[26] Hafiz, M. "Mechanical properties of SG-iron with different matrix structure."*Journal of materials science* 36(5) (2001): 1293-1300.

[27] Karsay, S. J. "The sorelmetal book of ductile iron." *Soremetal, Rio Tinto Iron & Titanum* (2004).

[28] Okabayashi, K., M. Kawamoto, A. Ikenaga, and M. Tsujikawa. "Impact characteristics and fractography of spheroidal graphite cast iron and graphite steel with hard eye structure." *Trans. Jpn. Foundrymen's Soc* (1982): 37-41.

[29] Wade, N., C. Lu, Y. Ueda, and T. Maeda. "Effect of distribution of second phase on impact and tensile properties of ductile cast iron with duplex matrix."*Trans. Jpn. Foundrymen's Soc.* 4 (1985): 22-26.

[30] Aranzabal, J., G. Serramoglia, and D. Rousiere. "Development of a new mixed (ferritic-ausferritic) ductile iron for automotive suspension parts." *International Journal of Cast Metals Research* 16(1-3) (2003): 185-190.

[31] Kocatepe, Kadir, Melika Cerah, and Mehmet Erdogan. "Effect of martensite volume fraction and its morphology on the tensile properties of ferritic ductile iron with dual matrix structures." *Journal of materials processing technology* 178(1) (2006): 44-51.

[32] Cerah, M., K. Kocatepe, and M. Erdogan. "Influence of martensite volume fraction and tempering time on tensile properties of partially austenitized in the (α+ γ) temperature range and quenched+ tempered ferritic ductile iron." *Journal of materials science* 40(13) (2005): 3453-3459.

[33] Erdogan, M., Kilicli, V., and Demir, B. "The influence of the austenite dispersion on phase transformation during the austempering of ductile cast iron having a dual matrix structure." *International Journal of Materials Research* 99(7) (2008): 751-760.

[34] Kilicli, Volkan, and Erdogan,M. "The strain-hardening behavior of partially austenitized and the austempered ductile irons with dual matrix structures."*Journal of materials Engineering and Performance* 17(2) (2008): 240-249.

[35] Druschitz, Alan, Ricardo Aristizabal, Edward Druschitz, Camden Hubbard, and Thomas Watkins. *Neutron Diffraction Studies of Intercritically Austempered Ductile Irons*. No. 2011-01-0033. SAE Technical Paper, 2011.

[36] Aristizabal, R., R. Foley, and A. Druschitz. "Intercritically austenitized quenched and tempered ductile iron." *International Journal of Metalcasting* 6(4) (2012).

[37] Aristizabal, R., Alan Druschitz, Edward Druschitz, R. Bragg, Camden R. Hubbard, Thomas R. Watkins, and M. Ostrander. *Intercritically Austempered Ductile Iron*. Oak Ridge National Laboratory (ORNL); High Flux Isotope Reactor; High Temperature Materials Laboratory, 2011.

[38] Garcia, C. I., and A. J. DeArdo. "Formation of austenite in 1.5 pct Mn steels."*Metallurgical Transactions A* 12(3) (1981): 521-530.

[39] Geib, Mark D., David K. Matlock, and George Krauss. "The effect of intercritical annealing temperature on the structure of niobium microalloyed dual phase steel." *Metallurgical Transactions A* 11(10) (1980): 1683-1689.

[40] Yi, Joon Jeong, In Sup Kim, and Hyung Sup Choi. "Austenitization during intercritical annealing of an Fe-C-Si-Mn dual-phase steel." *Metallurgical Transactions A* 16(7) (1985): 1237-1245.

[41] Speich, G. R., V. A. Demarest, and R. L. Miller. "Formation of austenite during intercritical annealing of dual-phase steels." *Metallurgical Transactions A* 12(8) (1981): 1419-1428.

[42] Mao-Shan, Li, and Zhang Ke-Jian. "New Development of Quenching Medium for Heat Treatment." *Heat Treatment of Metals* (1999): 04.

[43] Chen, C-H., and J-E. Zhou. "Measurement and application of cooling power of quenchants." *Heat Treatment of Metals(China)(China)* 11 (2001): 28-31.

[44] Sarwar, M., E. Ahmad, K. A. Qureshi, and T. Manzoor. "Influence of epitaxial ferrite on tensile properties of dual phase steel." *Materials & design* 28(1) (2007): 335-340.

[45] Huppi, G. S., D. K. Matlock, and G. Krauss. "An evaluation of the importance of epitaxial ferrite in dual-phase steel microstructures." *Scripta Metallurgica* 14(11) (1980): 1239-1243.

[46] Granbom, Ylva. "Structure and mechanical properties of dual phase steels: An experimental and theoretical analysis." (2010).

[47] Demir, B., and M. Erdoğan. "The hardenability of austenite with different alloy content and dispersion in dual-phase steels." *Journal of materials processing technology* 208(1) (2008): 75-84.

[48] Krauss, George. "Steels: heat treatment and processing principles." *ASM International, 1990,* (1990): 497.

[49] Lei, T. C., H. P. Shen, and J. Zhang. "Phase-Hardening and Phase-Softening Phenomena in Dual-Phase Steels." In *Proceedings of the International Conference on Martensitic Transformations. ICOMAT-86* (1986): 465-470.

[50] Steven, W., and A. G. Haynes. "The temperature of formation of martensite and bainite in low-alloy steels." *Journal of the Iron and Steel Institute* 183(8) (1956): 349-359.

[51] Krauss, G., Grossmann, M. A., and Bain, E.C. "Principles of heat treatment of steel." (1980).

[52] Zhao, Xi-Qing, P. A. N. Tao, Qing-Feng Wang, S. U. Hang, Cai-Fu Yang, and Qing-Xiang Yang. "Effect of tempering temperature on microstructure and mechanical properties of steel containing Ni of 9%." *Journal of Iron and Steel Research, International* 18(5) (2011): 47-58.

[53] Hernandez, VH Baltazar, S. S. Nayak, and Y. Zhou. "Tempering of martensite in dual-phase steels and its effects on softening behavior." *Metallurgical and Materials Transactions A* 42(10) (2011): 3115-3129.

[54] Kayali, Yusuf, Sukru Taktak, Sinan Ulu, and Yilmaz Yalcin. "Investigation of mechanical properties of boro-tempered ductile iron." *Materials & Design* 31(4) (2010): 1799-1803.

[55] Kobayashi, T., and H. Yamamoto. "Transformation induced plasticity in austempered low alloyed ductile iron." *Transactions of the Japan Foundrymen's Society* 8 (1989): 30-34.

[56] Sayed, A. Anazadeh, and Sh Kheirandish. "Affect of the tempering temperature on the microstructure and mechanical properties of dual phase steels."*Materials Science and Engineering: A* 532 (2012): 21-25.

[57] Zum Gahr, K-H. "Wear by hard particles." *Tribology International* 31(10) (1998): 587-596.

[58] Jacobson, Staffan, Per Wallén, and Sture Hogmark. "Fundamental aspects of abrasive wear studied by a new numerical simulation model." *Wear* 123(2) (1988): 207-223.

[59] Sahin, Y., M. Erdogan, and M. Cerah. "Effect of martensite volume fraction and tempering time on abrasive wear of ferritic ductile iron with dual matrix." *Wear* 265(1) (2008): 196-202.

[60] Zimba, J., M. Samandi, D. Yu, T. Chandra, E. Navara, and D. J. Simbi. "Un-lubricated sliding wear performance of unalloyed austempered ductile iron under high contact stresses." *Materials & design* 25(5) (2004): 431-438.

[61] Sahin, Y., M. Erdogan, and V. Kilicli. "Wear behavior of austempered ductile irons with dual matrix structures." *Materials Science and Engineering: A* 444(1) (2007): 31-38.

[62] Movahed, P., S. Kolahgar, S. P. H. Marashi, M. Pouranvari, and N. Parvin. "The effect of intercritical heat treatment temperature on the tensile properties and work hardening behavior of ferrite–martensite dual phase steel sheets."*Materials Science and Engineering: A* 518(1) (2009): 1-6.

[63] Aprameyan, S., and U. N. Kempaiah. "Dry Sliding Wear Behaviour of Ferrite-Martensite Dual Phase Steels." In *International Journal of Engineering Research and Technology*, 2(10) (2013).

[64]. Basso, A., R. Martínez, and J. Sikora. "Influence of chemical composition and holding time on austenite (γ) → ferrite (α) transformation in ductile iron occurring within the intercritical interval." *Journal of Alloys and Compounds* 509(41) (2011): 9884-9889.

[65] Ovali, Ismail, Volkan Kilicli, and Mehmet Erdogan. "Effect of microstructure on fatigue strength of intercritically austenitized and austempered ductile irons with dual matrix structures." *ISIJ international* 53(2) (2013): 375-381.

[66] Hernandez, VH Baltazar, S. S. Nayak, and Y. Zhou. "Tempering of martensite in dual-phase steels and its effects on softening behavior." *Metallurgical and Materials Transactions A* 42(10) (2011): 3115-3129.

[67] Kocatepe, Kadir, Melika Cerah, and Mehmet Erdogan. "The tensile fracture behaviour of intercritically annealed and quenched+ tempered ferritic ductile iron with dual matrix structure." *Materials & design* 28(1) (2007): 172-181.

[68] Das, Debdulal, and Partha Protim Chattopadhyay. "A Study on the effect of Martensite Morphology on Mechanical Properties of High-Martensite Dual-Phase Steels." (2002): 1-12.

[69] Offor, P. O., C. C. Daniel, and D. O. N. Obikwelu. "Effects of Various Quenching Media on the Mechanical Properties of Intercritically Annealed 0.15 wt% C–0.43 wt% Mn Steel." *Nigerian Journal of Technology* 29(2) (2010): 76-81.

[70] Tavares, S. S. M., P. D. Pedroza, J. R. Teodosio, and T. Gurova. "Mechanical properties of a quenched and tempered dual phase steel." *Scripta Materialia* 40(8) (1999): 887-892.

[71] Zhang, Jiecen, Hongshuang Di, Yonggang Deng, and R. D. K. Misra. "Effect of martensite morphology and volume fraction on strain hardening and fracture behavior of martensite–ferrite dual phase steel." *Materials Science and Engineering: A* 627 (2015): 230-240.

[72] Kamp, A., S. Celotto, and D. N. Hanlon. "Effects of tempering on the mechanical properties of high strength dual-phase steels." *Materials Science and Engineering: A* 538 (2012): 35-41.

[73] Gündüz, Süleyman. "Effect of chemical composition, martensite volume fraction and tempering on tensile behaviour of dual phase steels." *Materials Letters* 63(27) (2009): 2381-2383.

[74] Sirinakorn, Thipwipa, Vitoon Uthaisangsuk, and Sompong Srimanosaowapak. "Effects of the tempering on mechanical properties of dual phase steels."*Journal of Metals, Materials and Minerals* 24(1) (2014).

[75] Dieter, George Ellwood, and David Bacon. *Mechanical metallurgy*. Vol. 3. New York: McGraw-Hill, 1986.

[76] Manoj, Manoranjan Kumar, Vivek Pancholi, Sumeer Kumar Nath, S. Venkatesulu, L. Hemasundar, M. Sreeja, K. Divya et al. "Mechanical Properties and Fracture Behavior of Medium Carbon Dual Phase Steels." (2014).

[77] Sahin, Yusuf, Volkan Kilicli, Melika Ozer, and Mehmet Erdogan. "Comparison of abrasive wear behavior of ductile iron with different dual matrix structures."*Wear* 268(1) (2010): 153-165.

[78] Abouei, V., H. Saghafian, Sh Kheirandish, and Kh Ranjbar. "A Study on the Wear Behaviour of Dual Phase Steels." *Journal of Material Science Technology* 23(1) (2007).

[79] Perez, M. J., M. M. Cisneros, and H. F. Lopez. "Wear resistance of Cu–Ni–Mo austempered ductile iron." *Wear* 260(7) (2006): 879-885.

[80] Coronado, J. J., A. Gómez, and A. Sinatora. "Tempering temperature effects on abrasive wear of mottled cast iron." *Wear* 267(11) (2009): 2070-2076.

[81] Lu, Zhen-Lin, Yong-Xin Zhou, Qi-Chang Rao, and Zhi-Hao Jin. "An investigation of the abrasive wear behavior of ductile cast iron." *Journal of Materials Processing Technology* 116(2) (2001): 176-181.

[82] Modi, O. P., Pallavi Pandit, D. P. Mondal, B. K. Prasad, A. H. Yegneswaran, and A. Chrysanthou. "High-stress abrasive wear response of 0.2% carbon dual phase steel: Effects of microstructural features and experimental conditions."*Materials Science and Engineering: A* 458(1) (2007): 303-311.

……

Appendix -1

(a) Development of microstructure as-cast ductile iron

The microstructure of as-cast ductile iron mainly depends on the carbon content, the alloy and impurity content, ability of cast iron for nucleation and the solidification rate. These variables control the condition of the carbon and also its physical form. Eutectic cells are the elementary units for graphite nucleation. The cells solidify from the separate nuclei, which are basically graphite but also nonmetallic inclusions such as oxides and sulphides as well as defects and material discontinuities. Cell size depends on the nucleation rate in the cast iron. When the cooling rate and the degree of undercooling increase, the number of eutectic cells also increases, and their microstructure changes, promoting radial-spherical shape. The formation of graphite nodules is achieved by the addition of nodulizing elements, most commonly magnesium and, less often now, cerium. Higher silicon contents, reduces the potentials for eutectic carbides during solidification and promotes the formation of ferrite during slow solidification rate which results in the formation of as-cast ductile iron consisting of graphite nodules embedded in ferrite matrix.

(b) Development of microstructure of intercritical heat treated ductile cast iron

The range of silicon added is sufficient that the iron-carbon binary phase diagram is insufficient to predict the phases and microstructures that form. Since the Si content of the alloy selected for this investigation is about 2% the Fe-C-Si ternary diagram at 2% Si is presented below indicating the lower critical temperature (LCT) and upper critical temperature (UCT) and the phase co-existing below LCT, in the range of LCT and UCT.

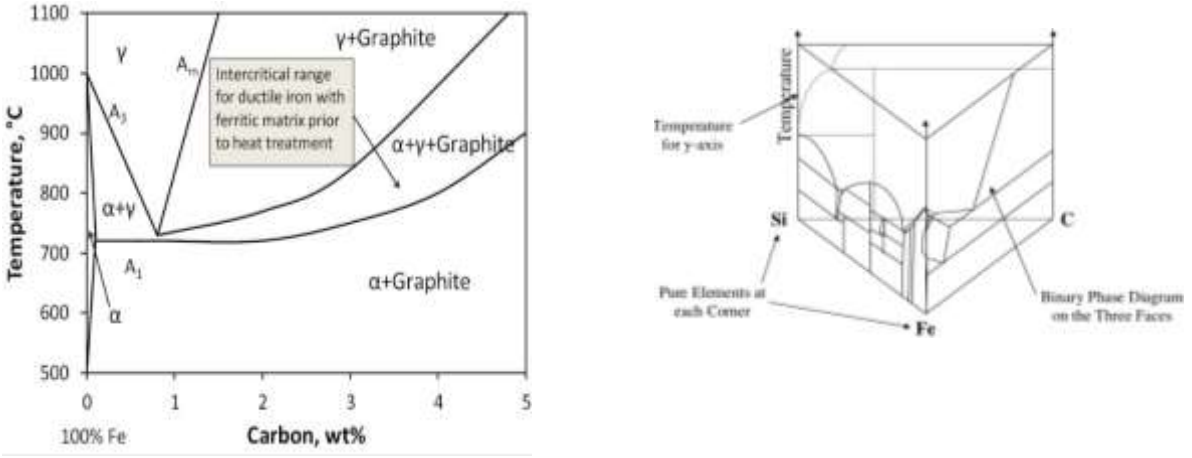

Figure 2.1 Iron-Carbon-Silicon (2%) Ternary Phase Diagram

An intercritical heat treatment starts with partial austenitization in the intercritical region where ferrite and austenite are present. The ICAT of the heat treatment plays a major role in the final microstructure of the material and therefore the mechanical properties. For a given alloy chemistry, the volume fraction of austenite is determined by the ICAT. It can be deduced from the iron-carbon-silicon ternary diagram at 2% Si using the lever rule that increasing the ICAT

increases the amount of austenite and decreases the amount of ferrite. Therefore, the ICAT step determines the amount of austenite transformation products in the final microstructure. On heating the as-cast matrix structure to the ICAT, the austenite at high temperature started to nucleate at the eutectic cells, which occurred because during the solidification process the manganese (which is an austenite stabilizing element) segregates to the eutectic cells, and favors the nucleation of the austenite in these regions. The areas surrounding the graphite nodules were mostly ferritic. This result was attributed to segregation of silicon (which is a ferrite stabilizer) during the solidification process to the areas surrounding the graphite nodules. The parent austenite formed during intercritical austenitizing transforms into martensite upon quenching. The quenching of the samples from different ICAT produced DMS with different ferrite and martensite volume fraction.

Appendix -2

Table 1.1 Modern casting census of world casting production

Year	Total Casting Tonnage of Alloys (Millions of Metric Tons)			
	Grey Iron	Ductile Iron	Aluminum	Steel
2004	40.30	18.30	10.22	6.20
2005	40.60	19.30	11.50	8.90
2006	42.50	21.40	11.83	9.80
2007	44.65	22.50	12.60	9.81
2008	42.49	23.70	10.92	10.18
2009	37.68	19.75	10.40	8.90
2010	42.80	23.14	10.90	9.64
2011	45.90	24.40	12.80	9.87
2012	45.60	25.00	13.80	10.75
2013	47.60	24.75	14.90	10.73

Table 4.3 Dependence of ferrite, martensite and graphite volume fraction on ICAT

Specimen Code	Ferrite volume fraction %	Martensite volume fraction %	Graphite volume fraction %
A785O	43	33	24
A785W	36	47	17
A815O	32	42	26
A815W	30	55	15

Table 4.6 Dependence of martensite microhardness on ICAT

Specimen code	Martensite microhardness (HV)
A785O	509
A785W	522
A815O	596
A815W	656

Table 4.7 Dependence of UTS, YS, %Elongation and Hardness on ICAT and quenching media.

Specimen code	ICAT °C	Quenching media	UTS MPa	YS MPa	Elongation %	Hardness HV50
A785O	785	Oil	520	162	12.45	421
A785W	785	Water	564	204	11.01	515
A815O	815	Oil	538	184	11.8	484
A815W	815	Water	609	223	10.36	572

Table 4.8 Dependence of UTS, YS, %Elongation and Hardness on tempering temperature

Specimen code	Tempering temperature °C	UTS MPa	YS MPa	Elongation %	Hardness HV50
A785O-T400	400	443	157	16.8	398
A785O-T450	450	436	144	17.24	372
A785O-T500	500	425	128	20.3	369
A785W-T400	400	472	179	11.84	509
A785W-T450	450	451	212	14.36	498
A785W-T500	500	448	155	17.2	428
A815O-T400	400	452	173	13.6	472
A815O-T450	450	450	151	16.01	434
A815O-T500	500	443	143	19.23	412
A815W-T400	400	532	182	11.47	555
A815W-T450	450	518	169	15.6	536
A815W-T500	500	511	165	17.8	511

Table 4.11 Dependence of weight loss on ICAT, quenching media and applied load.

Specimen code	Weight loss (gram) at respective loads		
	20N	40N	60N
A785O	0.005	0.018	0.026
A785W	0.003	0.013	0.016
A815O	0.003	0.014	0.021
A815W	0.002	0.007	0.013

Table 4.11 Dependence of weight loss on tempering temperature and applied load

Specimen code	Weight loss (gram) at respective loads		
	20N	40N	60N
A785O-T400	0.005	0.023	0.033
A785O-T450	0.006	0.027	0.041
A785O-T500	0.007	0.028	0.051
A785W-T400	0.004	0.016	0.029
A785W-T450	0.004	0.017	0.032
A785W-T500	0.005	0.027	0.046
A815O-T400	0.004	0.017	0.024
A815O-T450	0.004	0.026	0.032
A815O-T500	0.005	0.030	0.035
A815W-T400	0.002	0.018	0.020
A815W-T450	0.002	0.019	0.020
A815W-T500	0.003	0.019	0.025

List of Publications and Conferences

1. Influence of intercritical austenitizing temperature and different quenching medium on mechanical properties and wear behaviour of dual matrix structured ductile iron

Author: **Y H Mozumder**; R K Behera; S Sen
Published: 2015
Publication type: Scientific Journal article (Orissa Journal of Physics, ISSN 0974—8202) - peer reviewed.

2. Dry Sliding Wear System Response of Ferritic and Tempered Martensitic Ductile Iron

Author: **Y H Mozumder**; V K Jha; S Shama; R K Behera; A Pattaniak; Sindhoora L P; S C Mishra; S Sen
Published: 2015
Publication type: IOP Conference Series: Material Science and Engineering 75 (2015) 012009 - peer reviewed.

3. Adhesive Wear Behaviour of Heat treated SG Iron

Author: M Salim ; **Y H Mozumder**;; S Shama; R K Behera; A Pattaniak; Sindhoora L P; S C Mishra; S Sen
Published: 2015
Publication type: IOP Conference Series: Material Science and Engineering 75 (2015) 012003 - peer reviewed

4. Influence of Austenitizing Temperature and Quenching Medium on Wear Behaviour of Dual Matrix Structured Ductile Iron

Conference: National Metallurgist's Day 2014- Indian Institute of Metals, Pune, India

5. Dry Sliding Wear System Response of Ferritic and Tempered Martensitic Ductile Iron

Conference: National Conference on Processing & Characterization of Materials 2014 NIT Rourkela, India

……

Bio Data

Name	Yahya Hoque Mozumder
Date of Birth	19.05.1990
Permanent Address	H/N 10, AK Azad Road Satgaon Noapra, Panjabari Guwahati Assam India Pin: 781037
E-mail ID	yahyahoque@gmail.com
Languages Known	English, Hindi, Assamese, Bengali

Educational Qualifications:

Year	Degree/Certificate	Institution	Marks obtained
2012	Bachelor of Engineering (Mechanical Engineering)	Annamalai University, Tamil Nadu	CGPA 8.03 out of 10
2008	10+2 (AHSEC, Assam)	Swadeshi Academy, Guwahati, Assam	81%
2006	10 (SEBA, Assam)	Markaz Academy, Hojai, Assam	68.66%